AGU100 ADVANCING EARTH AND SPACE SCIENCE

JGR

Journal of Geophysical Research: Earth Surface

RESEARCH ARTICLE

10.1029/2017JF004489

Geomorphology of Scour Holes at Tidal Channel Confluences

Christian Ferrarin[1], Fantina Madricardo[1], Federica Rizzetto[1], William Mc Kiver[1], Debora Bellafiore[1], Georg Umgiesser[1,2], Aleksandra Kruss[1], Luca Zaggia[1], Federica Foglini[3], Alessandro Ceregato[1], Alessandro Sarretta[1], and Fabio Trincardi[3]

[1]ISMAR-Institute of Marine Sciences, CNR-National Research Council, Venice, Italy, [2]Open Access Centre for Marine Research, Klaipėda University, Klaipėda, Lithuania, [3]ISMAR-Institute of Marine Sciences, CNR-National Research Council, Bologna, Italy

Key Points:
- Twenty-nine scours in a depth range between 7 and 26 m are found at tidal channel confluences in the Venice Lagoon
- Scour depth positively correlates to the tidal prism of the confluent channels
- Historical datasets revealed the century-scale morphodynamics of these erosive features, as a consequence of changes in the flow regime

Correspondence to:
C. Ferrarin,
c.ferrarin@ismar.cnr.it

Citation:
Ferrarin, C., Madricardo, F., Rizzetto, F., Mc Kiver, W., Bellafiore, D., Umgiesser, G., et al. (2018). Geomorphology of scour holes at tidal channel confluences. *Journal of Geophysical Research: Earth Surface*, *123*, 1386–1406. https://doi.org/10.1029/2017JF004489

Received 8 SEP 2017
Accepted 16 MAY 2018
Accepted article online 24 MAY 2018
Published online 19 JUN 2018

Abstract The morphology of scour holes at tidal channel confluences was investigated through high-resolution acoustic mapping of the channel network in the Venice Lagoon (Italy). Our investigation identified 29 confluence scours ranging in depth from 7 to 26 m and characterized by different confluence geometry and scour properties. Scours were found at the confluence of two or more channels, having equal or unequal bed heights and a diverse confluence planform geometry. The main morphological characteristics of the scours were compared to literature data from fluvial environments. Like in rivers, the scour depth tends to increase with the angle of the confluence. Moreover, the maximum depth of the confluence scours in the Venice Lagoon is positively correlated with the tidal prism of the channels joining the confluence. The investigation of the seafloor features in the scour holes highlighted that, generally, small- and medium-scale bedforms are present on the gentle slope. The scours' seafloor roughness indicated that in tidal channels both ebb and flood flows combine in shaping the confluence morphology. In addition, the analysis of historical bathymetric datasets dating back to the 1800s allowed us to analyze the morphological evolution of two of these erosive features. Our findings revealed the century-scale morphological dynamics of scour holes, as a consequence of changes in the flow regime.

1. Introduction

Tidal channel networks exert a crucial control on water, sediment, pollutant, and nutrient exchanges within coastal wetlands and deltas (A. D'Alpaos et al., 2005; Hoitink et al., 2017), some of the most valuable ecosystems on the planet with ecological, historical, economical, and social relevance (Pérez-Ruzafa et al., 2011; Perillo et al., 2009; Wolanski & Elliott, 2015). Even if there are many analogies between channel networks in tidal environments and rivers, several morphological features of the tidal channels show strong variations in space that are unusual in fluvial morphology (Fagherazzi et al., 1999, 2004). However, like rivers, tidal channels also have deep scours, that is, depressions in the channel bed caused by erosion processes induced by the hydrodynamic conditions. Scour holes in rivers are generally found at channel confluences, critical nodes in river networks where a tributary channel enters the river mainstream (Ashmore & Parker, 1983; Best, 1986, 1988; Best & Ashworth, 1997; Best & Rhoads, 2008; Biron et al., 1993; Mosley, 1976, 1982; Rice et al., 2008; Sambrook Smith et al., 2005).

Even if scour holes are recognized to be common features also in tidal embayments with confluent channels, few studies on the morphology of these erosive structures in natural tide-dominated systems can be found in literature: Kjerfve et al. (1979) investigated the origin of scour holes in the tidal creeks of the coastal South Carolina, while Ginsberg and Perillo (1999) and Ginsberg et al. (2009) examined morphodynamics and seismostratigraphy of scours in the Bahia Blanca Estuary (Argentina). Recently, Fraccascia et al. (2016) highlighted the presence of a deep confluence scour when analyzing sediment transport and bedform migration in the Danish Wadden Sea (Denmark).

In comparison with rivers, flow and sediment dynamics at tidal channels are complicated by the flood/ebb alternation of the tidal currents. A number of studies investigated the dynamics in tidal channel confluences, shedding some light on the relative effects of the scours and channels' geometry, the tidal cycle, and the density gradients. Pierini et al. (2005) investigated a natural confluence of channels in the inner Bahìa Blanca Estuary and found that the junction produces a distortion of the vertical flow and variations in the suspended

sediment transport. Buschman et al. (2013) reported on observations during a tidal cycle of a stratified triple tidal junction in an Indonesian tidal system. They showed the driving effect of bathymetric differences between the channels, with consequent modification of tidal propagation (amplitude and phase) and flow. Buschman et al. (2013) also stated the role of tides and baroclinic gradients in defining hydrodynamics and sediment division linking these effects to morphological changes. Salas-Monreal and Valle-Levinson (2009) studied two estuarine hollows in the lower Chesapeake Bay, focusing on the flow characteristics during flood and ebb tide. During the flood phase, they observed an acceleration at midwater depth caused by convergence of lateral flows at the entrance of the scour, while there was a flow divergence at the exit of the scour with subsequent weakening of the flow. Also, the major role of advective forces over the scour is reported, while friction seems to dominate along the shoals. Finally, the Coriolis force tends to increase horizontal dynamic asymmetry over large enough scours (Cheng & Valle-Levinson, 2009). This dynamics is also influenced and modified by density fronts, as mentioned in Cheng and Valle-Levinson (2009). Moreover, according to Li and Zheng (2016), large vertical accelerations characterize the flow over the steep sides of a scour hole, suggesting that the motion may be nonhydrostatic. Deviation from the hydrostatic pressure distribution and strong vertical flow acceleration were also found near the scour in a sharp bend along the Mahakam River (Vermeulen et al., 2015).

The present study is based on an unprecedented extensive mapping of a tidal network in a microtidal coastal environment (Madricardo et al., 2017). The high-resolution bathymetric data acquired in 2013 in the Venice Lagoon (Italy) allowed a detailed description of the geomorphological characteristics of scour holes at channel confluences. Our aim is to use the knowledge available on river confluences to understand the morphodynamics of scour holes at tidal channel junctions.

In fluvial systems and coastal areas, man has become one of the major geomorphological agents, determining substantial changes in the characteristics of the Earth's physical landscapes (Hoitink et al., 2017; Hooke et al., 2012; Maselli & Trincardi, 2013; Rhoads et al., 2016; Syvitski et al., 2009). The Venice Lagoon was subjected to several human modifications that altered the hydrodynamics in the tidal channel network (Carniello et al., 2009; D'Alpaos, 2010; Ferrarin et al., 2015; Sarretta et al., 2010; Tambroni & Seminara, 2006). As several historical bathymetric maps are available, it is therefore an ideal site for studying the long-term morphological evolution of scours at channel confluences.

The objectives of the research here described are to (i) map scour holes at channel junctions in the Venice Lagoon, (ii) examine their geomorphological characteristics and compare them with scours in rivers, (iii) explore the high-resolution bathymetry to investigate the seafloor features in the scour holes, and (iv) study their century-scale morphological evolution using historical bathymetric datasets.

1.1. Study Site

The Venice Lagoon is situated in the Northern Adriatic Sea (Figure 1) and is one of the largest Mediterranean lagoons (area of 550 km^2). Even if the lagoon is a microtidal system (tidal range of about 80 cm), tides are a major factor in shaping landforms and driving ecological gradients and biological communities. The lagoon is separated from the open sea by barrier islands, and three inlets (Lido, Malamocco, and Chioggia) ensure an active renewal of the lagoonal waters (Ferrarin et al., 2010). The lagoon is characterized by a complex system of tidal channels. The density of the drainage network increases landward as main tidal collectors departing from the inlets branch in progressively smaller-size channels, ranging in depth from a more than 15 m of main reaches to a few centimeters of salt marsh creeks. Such a drainage network cuts across a large extent of shallow water areas, which have an average depth of 1 m and include mud flats and salt marshes.

The Venice Lagoon formed around the end of the Holocene transgression, which reached its maximum 8/7 and 6 kyr BP in the southern and central lagoon, respectively (Madricardo et al., 2012; Storms et al., 2008; Zecchin et al., 2008). The transgressive sediments lay above an overconsolidated clay layer, representing the last continental pedogenized Pleistocene deposit (Donnici et al., 2011). This altered alluvium, locally called *caranto*, extends heterogeneously under the lagoon and currently has a thickness ranging from a few meters to only a few centimeters due to depositional conditions, diagenetic processes, or subsequent erosion. In the lagoon area, the depth of the caranto layer is not uniform but generally varies from about 1 m close to the landward northern margin to 18 m at the Chioggia inlet (Tosi et al., 2007a, 2007b). The caranto exhibits relatively high compressive and shear strength, thereby providing a substrate that, if exposed at the lagoon floor, may delay further erosional processes.

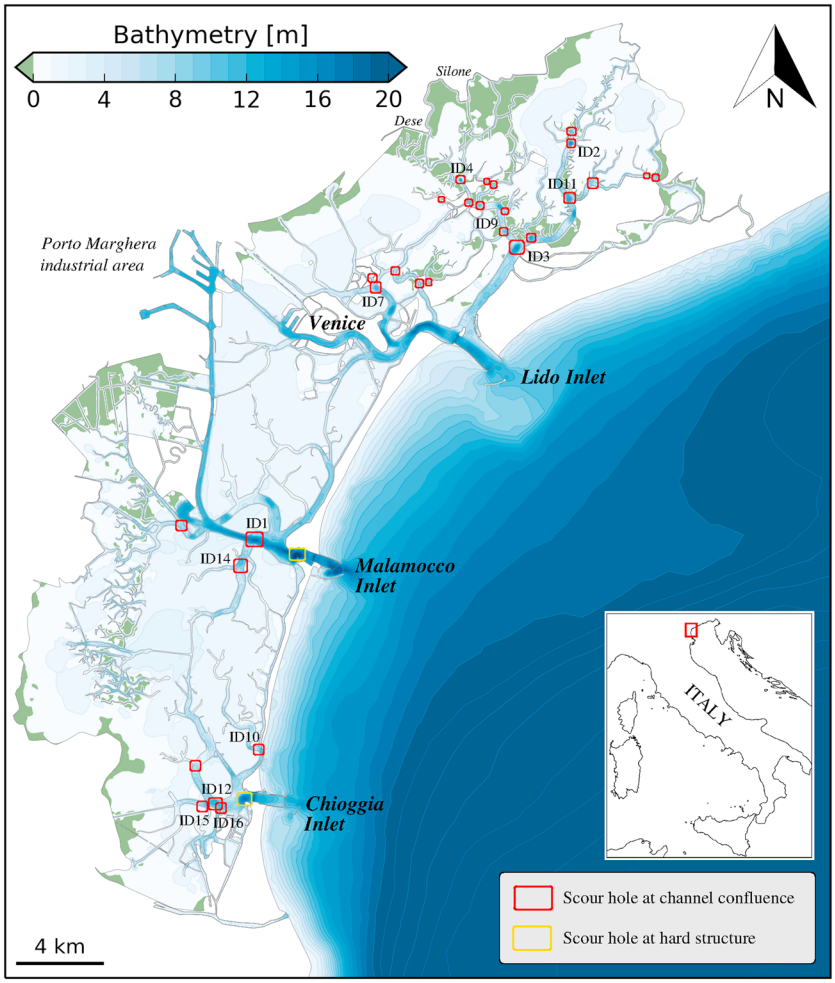

Figure 1. Bathymetry of the Venice Lagoon with marked scour holes. Identification numbers are reported only for channel confluences discussed in this paper.

The Holocene section includes shallow-marine deposits recording the latest stages of the postglacial sea level rise (Transgressive Systems Tract, according to Zecchin et al., 2008; Rizzetto et al., 2009) and a more recent section including delta plain, lagoonal, littoral, and shoreface to inner shelf deposits accumulated during the modern Highstand Systems Tract (Rizzetto et al., 2009; Zecchin et al., 2008). The distribution of surface sediment in the lagoon is affected by hydrodynamics and is characterized by coarser materials in the proximity of the inlets and tidal channels and finer materials in mudflats and salt marshes (Molinaroli et al., 2007). Channel bed materials also change following the hierarchy of distributaries with finer materials in creeks and coarser deposits at the bottom of the largest tidal collectors.

The morphological evolution of the Venice Lagoon has been strongly influenced by the presence of humans since the tenth century (L. D'Alpaos, 2010; Madricardo & Donnici, 2014; Zecchin et al., 2008). Analysis of past and recent landscapes has shown a drastic reduction of salt marsh extent and channel number over the centuries, as a result of relative sea level rise, as well as artificial diversion of rivers and modifications of the inlets (Madricardo & Donnici, 2014; Sarretta et al., 2010). As a consequence, from a highly complex, well-developed microtidal system, the lagoon was transformed into the high-energy-dominated, flatter-bottomed, and more open bay-like environment of today, where the simplified morphology and increased water depth favor water exchange with the sea.

2. Materials and Methods

2.1. Bathymetric DataSets

2.1.1. High-Resolution Multibeam Bathymetry

The most recent channel network bathymetry was collected from May to December 2013 with a Kongsberg EM-2040 compact dual-head multifrequency MultiBeam Echo Sounder (MBES) set at 360 kHz. The dual-head multibeam operated with a swath opening angle of 70° for each head inside the channels and 60° in the inlets, maintaining 15° of overlap between the two swaths. The MBES was pole-mounted on the CNR research vessel Litus, a 10-m-long boat with 1.5-m-deep draft. The vessel sailed with a reasonably constant speed (mean speed 4 knt). The 2013 dataset was collected with a 40% overlap between acquisition lines, thus covering the full channel bed with a 0.5-m resolution.

The positioning system was a Seapath 300 supplied by a Fugro HP Differential Global Positioning System, with horizontal accuracy of 0.2 m. The motion sensor MRU 5 by Kongsberg and a Dual Antenna Global Positioning System integrated in the Seapath corrected pitch, roll, heave, and yaw movements (reaching 0.02° roll and pitch accuracy and 0.075° heading accuracy). The sound velocity was measured continuously with a Valeport mini sensor attached close to the transducers. Sound velocity profiles were systematically collected with an AML oceanographic Smart-X sound velocity profiler.

The collected raw MBES data were cleaned, tidally corrected, adjusted for motion sensor offsets, and gridded with the software CARIS HIPS, version 7, and SIPS, version 9.1 (CARIS HIPS and SIPS, 2013), taking into account sound velocity profiles. A set of 93 virtual tidal stations, evenly distributed in the study area, served for tidal correction: a virtual tidal station was used for each field sheet in CARIS created for the data collected in a single day of survey. The tidal corrections in each virtual tidal station were calculated using the water level simulated by the hydrodynamic model SHYFEM (Umgiesser et al., 2004) applied to the whole Venice Lagoon with assimilation of tide gauge observations. The final bathymetry was created with the Swath Angles Weighting option with a Max Footprint size of 9×9 pixels and a resolution of 0.5 m and cleaned using the subset editor to handle and visualize efficiently the data. The reader is referred to Madricardo et al. (2017) for a full description of the instrumental setup and raw data access and processing protocols.

2.1.2. Historical DataSets

The historical bathymetric datasets used for assessing the morphological evolution of the scour holes in the Venice Lagoon were derived from the following:

1. the military topographic/hydrographic map of the lagoon by Augusto Denaix of circa 1810 composed of 35 map sheets (Magrini, 1933a). This is the first map of the Venice Lagoon drawn using the Cassini projection and based on a modern theoretical approach to geodetic measurements. The map provides the detailed bathymetry of the main channels and inlets, but not of the tidal flats. Depths were measured with a sounding line (rope with a lead plummet) and sounding rod (Zille, 1955).
2. the topographic/hydrographic map by the Genio Civile di Venezia of 1901 composed of 18 map sheets (Magrini, 1933b), reporting bathymetric data collected with sounding rod and sounding line (Zille, 1955);
3. the bathymetric map published by the Venice Water Authority (Magistrato alle Acque di Venezia, MAV) in 1934 as a result of a survey carried out between 1922 and 1933 (median year 1927) by performing precise tacheometric measurements and manual soundings. A precise altimetric network covered the entire lagoon surface;
4. the bathymetric dataset by MAV of 1970 (surveys carried out from 1968 to 1971). Bathymetric data were collected by multiple sampling methods: echosounding, tacheometric measurements, and stereo photogrammetric analysis for the shallowest reaches of the lagoon;
5. the bathymetric dataset by MAV of 2002, collected from 1999 to 2002 and further integrated with data collected in 2003. A multibeam bathymetric acquisition system was used for the main channels (depth >5 m) and the inlets. Unfortunately, only sparse bathymetric data extracted from the multibeam dataset along cross-channel transects were available. For shallow waters and secondary channels (depth <5 m), a single-beam echosounder was used.

For the analysis of the historical morphological evolution we focused on two selected areas located in the northern and southern lagoon, respectively. The first confluence is located north of the Lido inlet (ID3), whereas the second is located west of the Chioggia inlet (ID12), where a complex tidal channel junction has developed over the last centuries.

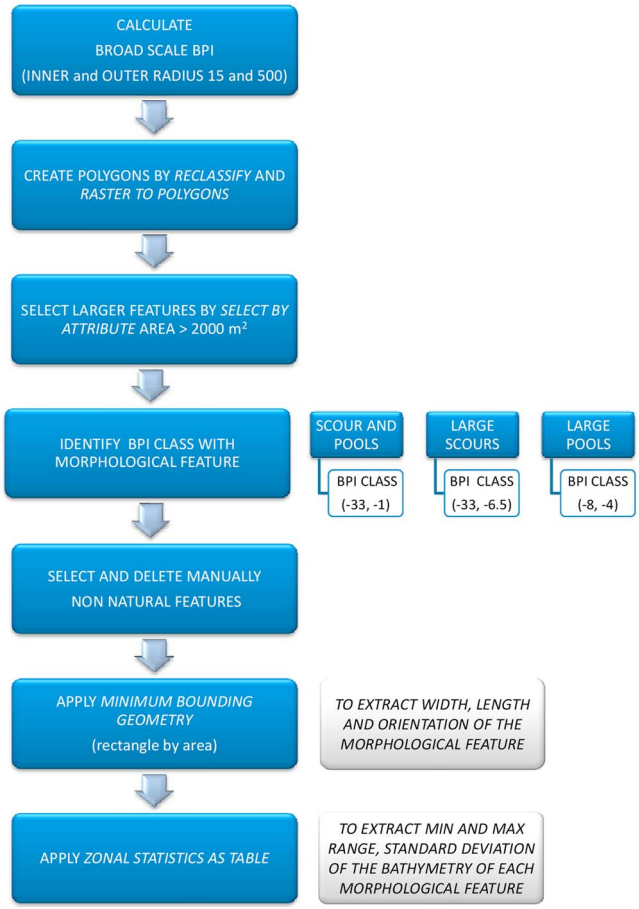

Figure 2. Workflow diagram of the procedure used for the identification of the confluence scours from the 2013 MBES dataset. MBES = multibeam echosounder; BPI = benthic position index.

The oldest bathymetric datasets were acquired from the 1810 and 1901 historical maps. The corresponding digital raster images of the map sheets (from 7 to 10 km per side) reporting the two areas of investigation were georeferenced using the software ArcGIS v.10.2. Even if these maps were very detailed, they were realized before the use of the aerial photographs and, consequently, only based on data from field work as well as descriptions and sketches produced during the surveys. In order to position the maps correctly in space, we identified several control points that remained unchanged over time (for scours ID3, 70, and 109 control points in the 1810 and 1901 maps, respectively; for scour ID12, 55, and 37 control points in the 1810 and 1901 maps, respectively). In the georeferencing process, the local transformation, based on an algorithm combining a polynomial transformation and triangulated irregular network interpolation techniques, was applied to minimize errors between the actual location of each selected point and its manual positioning (Balletti, 2006; Balletti et al., 2016). This method gave the best results, optimizing for both global least squares fitting and local accuracy. The 1927, 1970, and 2002 bathymetric datasets were provided by Sarretta et al. (2010).

Each analyzed dataset was referenced to the mean sea level (which in turn was referenced to the local datum) at the moment of the survey to obtain comparable total water depth values. The two oldest datasets (1810 and 1901), originally referred to the mean high tide, were converted to the mean sea level by subtracting 25 cm (L. D'Alpaos, 2010).

2.2. MBES Bathymetry Data Analysis

The identification of the confluence scours was carried out starting from the high-resolution MBES dataset of 2013. The 0.5-m resolution bathymetric data (Madricardo et al., 2017) were analyzed in ArcGIS v.10.2, following the workflow illustrated in Figure 2 and described below:

1. first we calculated the broad-scale Benthic Position Index (BPI) within the Benthic Terrain Modeller toolbox (Wright et al., 2012), setting the inner and outer radius to 15 and 500 raster cells, respectively. BPI indicates

the topographic positions of the cells, with negative values representing locations that are lower than their surroundings (valleys).
2. the resulting BPI raster values were grouped into three intervals (BPI ≤ -1, $-1 <$ BPI ≤ 1, BPI > 1) to identify the concave, flat, and convex areas, respectively. By using the Reclassify tool we reclassified the values of the raster smaller than −1 to 1 and the other values to NoData. Finally, we converted the resulting raster into polygons with the Raster to Polygon tool;
3. to select only large features, we retained only polygons with an area larger than 2,000 m^2 with the Select by Attributes tool;
4. then, we identified several erosive features as confluence scours and hollows at tidal channel meander bends (pools) within the polygons obtained from the BPI class ranging from −33 to −1. Within this class, BPI between −33 and −6.5 isolated the largest scours and BPI between −8 and −4 the largest pools, respectively.
5. among the identified scours, we manually selected the confluence scours eliminating the nonnatural features highlighted by the BPI calculation (i.e., dredging marks). In a few cases, the polygons were manually modified following the isobaths (ID02, ID05, and ID07);
6. we constructed the rectangles containing each scour by applying the Minimum Bounding Geometry tool with the Rectangle by area option. In this way, we could extract the width, length, and orientation with respect to north for each scour;
7. we finally applied the Zonal Statistics as Table algorithm in order to extract the minimum and maximum depths of each scour with the respective standard deviation. The confluence angle was measured manually from the bathymetric data with the help of satellite images as a background.

2.3. Uncertainty Estimation

Errors in bathymetric measurements arise from different sources, that is, installation offsets, instrument characteristics, position uncertainties, and timing errors. For the 2013 MBES dataset, the Total Propagated Uncertainty (TPU), which results from the combination of all individual error sources was calculated in CARIS HIPS and SIPS. TPU can be split into horizontal (hzTPU) and vertical (dpTPU) components, related to the positioning of each sounding and depth values uncertainties. Mean values obtained for the whole dataset are hzTPU = 0.4 m and dpTPU = 0.1 m (referred to 20-m depth, Madricardo et al., 2017).

Errors in depth values of the older datasets are difficult to assess since there is almost no documentation about the past acquisitions. For the 1810 and 1901 datasets the measurements in the deeper parts of the channels were undertaken during slack water. Assuming that the sounding line could have been at maximum inclined by 15°, we estimated a depth error of about 2% (De Marchi, 1913). The uncertainty of the 1927, 1970, and 2002 datasets was assumed to be higher than the one of the 2013 MBES survey. Therefore, to be conservative and considering the acquisition technique, we considered the error of the bathymetric data to be 0.5 m for the 1810 and 1901 datasets, 0.4 m for the 1927 dataset, 0.3 m for the 1970 dataset, and 0.2 m for the 2002 dataset (twice the error estimated for the 2013 MBES survey).

Due to lack of information, it was not possible to estimate the positioning errors of the older datasets, which present a spatially variable density of data and thus offer an incomplete coverage of the channel bottoms. To allow comparison between the different bathymetric maps, these datasets were interpolated (with a Triangulated Irregular Network interpolation type) on a regular grid of 2-m resolution. It is obvious that the number and distribution of the irregularly spaced bathymetric stations affect the reliability of the obtained gridded field. As the data from the old bathymetric maps do not lie on a regular grid, we used the 2013 swath bathymetry dataset in order to calculate the error introduced by the interpolation procedure. With this aim, the 2013 bathymetry data were resampled at the locations of observations of older datasets and five interpolated grids (with the same resolution of 2 m) were constructed. The comparison of these interpolated bathymetric datasets along selected transects allowed for the computation of the root-mean-square deviation associated with the gridding procedure of the sparse measurements.

3. Results

3.1. Mapping Confluence Scours in the Venice Lagoon

The bathymetric analysis procedure described in section 2.2 allowed the identification of 29 confluence scours in the channel network of the Venice Lagoon (squares in Figure 1). The majority of the confluence scours are located in the northern sector of the lagoon (referring to the Lido inlet), which is characterized by a wider

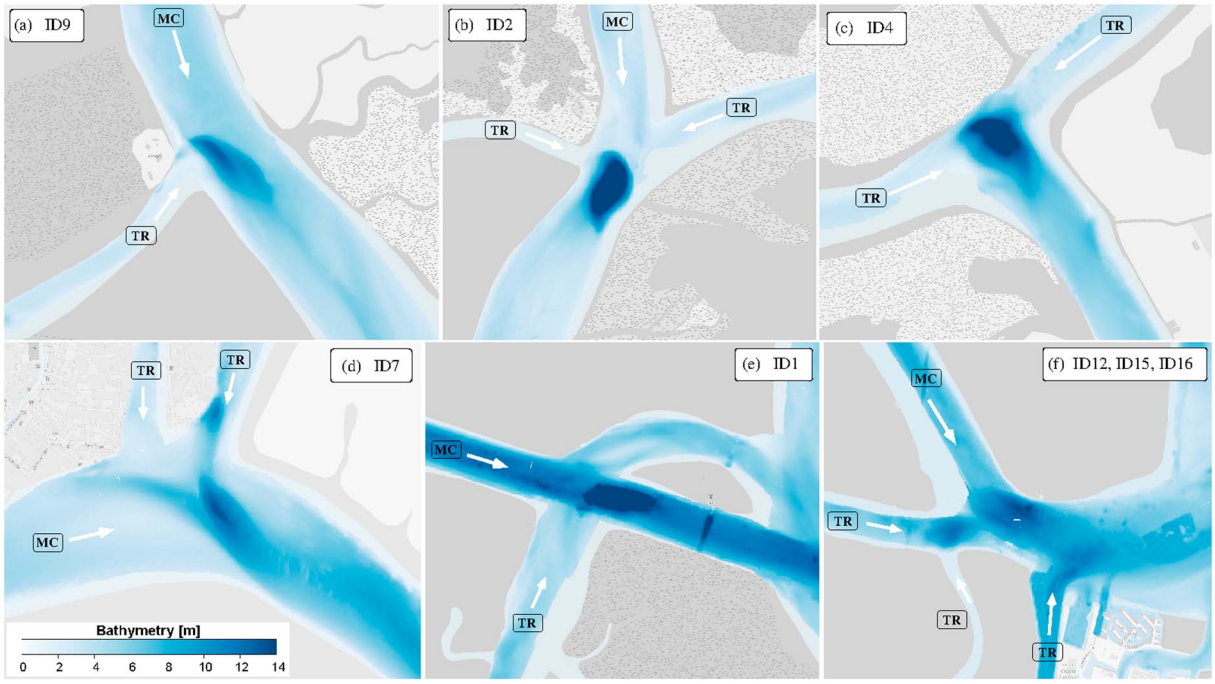

Figure 3. Examples of different tidal channel confluences with scour holes: (a) mainstream channel and one tributary (scour ID9); (b) mainstream channel and two tributaries (scour ID2); (c) wide-angle confluence of equal size streams (scour ID4); (d) confluence of two minor tributaries at a mainstream meander (scour ID7); (e) intersection between the artificial Malamocco-Marghera channel and a tributary (scour ID1); (f) junction of different tributaries with a mainstream channel (group of three adjacent scours, ID12, ID15 and ID16). MC and TR labels identify the mainstream and the tributary, respectively, with white arrows showing ebb flow direction. Background image from OpenStreetMap (http://www.openstreetmap.org).

morphological complexity and, consequently, a larger drainage density (Sarretta et al., 2010). Two additional scours, reaching depths of 29 and 48 m, were found at channel junctions close to the inner end of the southern jetty at the inlets of Chioggia and Malamocco, respectively (yellow squares in Figure 1). Because of the complex flow interactions with the jetty (flow contraction and generation of large vortices; Van Rijn, 1998), these features were not considered as scours at natural channel confluences and were not included in the analysis.

By mapping the scours at channel junctions, we observed a wide variety of confluence planform geometries (Figure 3). Consistent with river studies, we considered the ebb tide flow pattern to identify the tidal channels joining the confluence as upstream reaches. Twenty-four scours are found at the confluence of two upstream reaches (i.e., one mainstream and one tributary, see Figure 3a) and five scours are found at the confluence of three upstream channels (i.e., one mainstream and two tributaries, see Figure 3b). In the drainage network of the Venice Lagoon, however, it is not always easy to distinguish between the mainstream and the tributaries. An example is the channel junction ID4, where two secondary channels have almost identical size and depth as they join into a main channel (Figure 3c).

At the junction of two upstream reaches, the confluence angle ranges between 45° and 165°, with an average value of 111°. When three upstream reaches lead into the scour hole, the angle of confluence, considered as the wider angle between the upstream channels, ranges between 103° and 165°. Considering all junctions, the average value of confluence angles is 114°.

Due to the high sinuosity of the tidal channels (Fagherazzi et al., 1999), in 14 cases (see Figure 3d) the confluent upstream or downstream reaches possess a curvature. According to Roberts (2004), Riley and Rhoads (2012), and Riley et al. (2015), such a confluent meander bend may lead to differences in flow structure at the junction, affecting the scour shape and depth.

Since the Venice Lagoon is a heavily modified coastal environment, we also found scours at confluences with artificial channels. This is the case of the confluence scour ID1, the deepest depression found among the features, considered with a maximum depth of 26 m (Figure 3e). It is located at the intersection of the Malamocco-Marghera channel with a large tidal channel (split into two tributaries). The Malamocco-Marghera channel was opened in 1970 to connect the Malamocco Inlet with the industrial area of Porto Marghera

Table 1
Morphological Characteristics of the Identified Scour Holes at Channel Junctions in the Venice Lagoon in Terms of Scour Maximum Flow Depth, Main Channel Depth, Tributary Channel Depth, Relative Scour Depth, Scour Length, Number of Upstream Channels, Confluence Angle, Side of the Steep Face, and Presence of Meander Bend

ID	d_{max} (m)	MC depth (m)	TC depth (m)	d_r	Length (m)	*N* channel	Angle (deg)	Steep face	Meander bend
1	26.2	12.7	6.5	2.9	422.7	2	80	upstream	no
2	21.4	3.5	2.5	7.1	277.0	3	130	upstream	no
3	20.3	5.4	4.7	4.0	735.4	2	103	upstream	yes
4	17.6	3.0	2.7	6.2	163.6	2	156	upstream	no
5	16.0	5.2	4.1	3.3	141.2	2	135	upstream	yes
6	15.8	4.2	3.8	3.9	162.4	2	120	upstream	no
7	15.3	4.4	3.5	3.8	294.3	3	128	upstream	yes
8	15.0	3.1	3.2	4.9	302.6	2	91	upstream	no
9	14.8	4.8	2.1	3.5	306.5	2	119	upstream	no
10	14.6	3.4	4.0	4.1	386.3	3	103	downstream	yes
11	14.3	5.4	5.7	2.6	508.6	2	138	downstream	no
12	14.2	4.9	4.7	2.9	521.1	2	58	upstream	no
13	13.4	3.5	1.6	4.4	140.0	2	165	upstream	yes
14	12.2	4.3	3.8	3.0	412.9	2	67	downstream	yes
15	12.1	4.7	2.4	3.0	260.1	3	165	upstream	no
16	12.0	5.5	4.5	2.3	429.5	2	96	upstream	no
17	11.7	2.7	2.5	4.5	128.7	2	155	upstream	no
18	11.6	3.6	3.4	3.3	206.9	2	80	upstream	yes
19	11.5	4.0	2.7	3.2	66.5	2	100	upstream	yes
20	11.4	4.1	4.3	2.7	153.8	2	102	upstream	no
21	11.2	4.8	4.3	2.4	246.5	2	45	upstream	yes
22	10.5	3.2	2.6	3.6	156.6	2	120	upstream	no
23	10.3	5.0	3.5	2.4	170.7	2	102	upstream	yes
24	10.3	2.4	2.5	4.2	134.5	2	123	upstream	yes
25	9.5	3.2	2.3	3.5	148.2	2	117	upstream	no
26	9.2	3.7	2.4	2.9	269.8	2	160	downstream	yes
27	8.0	3.6	1.9	2.5	49.5	2	120	upstream	no
28	7.9	3.4	2.9	2.6	259.0	3	124	upstream	yes
29	7.1	3.4	1.4	2.4	94.5	2	112	upstream	yes

Note. Scours are ordered by descending maximum depth.

and is periodically dredged to allow navigation of a variety of ships including oil tankers, bulk carriers, cargo ships, and ferries. Therefore, this scour did not develop at a natural channel confluence.

The complex network of connecting branches produces in some cases closely spaced scours. This happens, for example, at the confluence of several reaches creating three adjacent scour holes (ID12, ID15, and ID16) connected together (Figure 3f).

The main morphological characteristics of the detected confluence scour holes are reported in Table 1. Additionally, the relative scour depth (d_r) is computed according to Ashmore and Parker (1983) and Sambrook Smith et al. (2005) as the ratio of the maximum flow depth of the scour hole (d_s) to the average flow depth (considering a 200-m-thick cross-channel band) of the upstream tidal reaches in proximity of the confluence (d_c) leading into the scour hole:

$$d_r = \frac{d_s}{\sum d_c / n}, \tag{1}$$

where n indicates the number of channels joining the confluence.

The 29 confluence scours identified in the investigated channel network have maximum flow depths (d_{max}) ranging from 7 to 26 m and a mean depth of 13 m. The relative scour depths (d_r) have values between 2.4

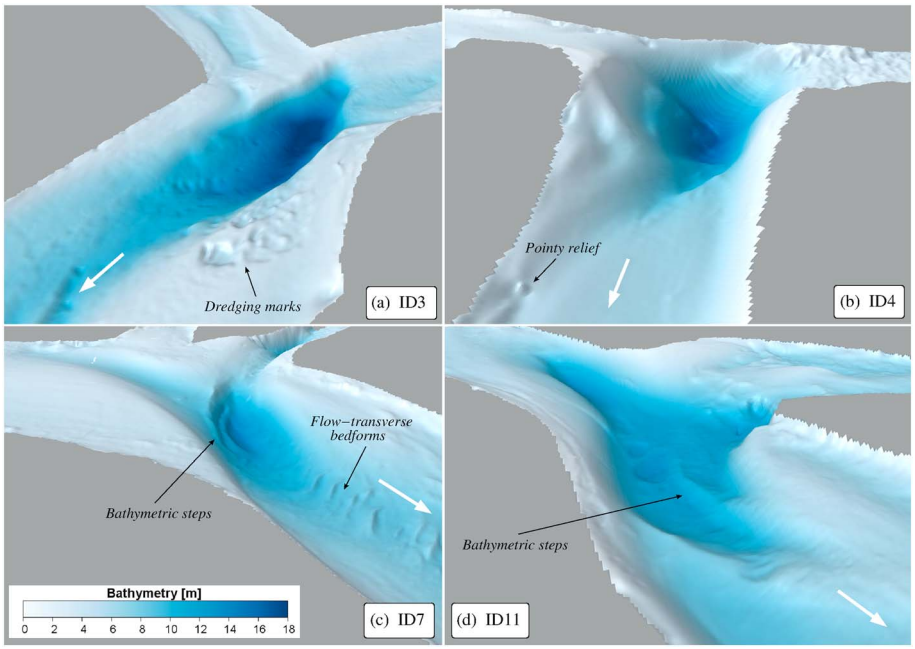

Figure 4. Three-dimensional digital bathymetric model of scour holes ID3 (a), ID4 (b), ID7 (c), and ID11 (d) with 4 times vertical exaggeration. White arrows indicate ebb flow direction.

and 7.1, with an average value of 3.5. The scours have lengths varying from 50 to 735 m, with the larger scours generally found at confluences of large channels.

Similar to scour holes in rivers and in other tidal systems (Ginsberg & Perillo, 1999; Kjerfve et al., 1979), the shape of the scour holes at tidal channel confluences in the Venice Lagoon is generally asymmetric. In most of the scours studied herein, the steep face of the hole is on the upstream side with respect to ebb direction (see Figures 4a and 4b as examples). As in fluvial environments (Keller, 1978), we locally observed the typical riffle and pools morphology of meandering channels. When the channel junction occurs in association with a meander bend, pool and confluence scour overlap. Therefore, the resulting scour hole extends upstream of the confluence in the curved main channel (Figure 4c). At confluence ID11, the scour develops also in the direction of the main upstream channel even without the presence of a meander (Figure 4d).

3.2. Seafloor Features in the Scour Holes

The maps reported in Figure 4 also provide a detailed overview of the channel bed ruggedness, highlighting the presence of several small-scale erosive and depositional features. The presence of flow-transverse bedforms was documented in 14 scour holes, mainly at confluences of large channels and close to the inlets where sediments are coarser. In these scour holes, the bedforms are located on the gentler side of asymmetric scours, whereas they are located on both sides of symmetric scours. For asymmetric scours, the bedforms are generally oriented seaward (Figure 4c).

The bedforms on the gentle side of the scours are three dimensional and their height (h) and wavelength (λ) is highly variable even within the same scour. We could measure h and λ ranging from $h = 0.1$ m and $\lambda = 3.5$ m to $h = 0.6$ m and $\lambda = 18$ m, up to the maximum of $h = 1$ m and $\lambda = 20$ m (Figure 4c).

The high resolution of the MBES bathymetric dataset also allows the identification of several unclassified bottom features, such as areas with a rapid change in bathymetry (the bathymetric steps at scours ID7 and ID11, Figures 4c and 4d), distinct elements probably generated by dredging activity (Figure 4a) and a pointy relief due to the presence of a wooden pile at the side of the channel (Figure 4b).

Analyzing the bathymetry profiles along all scours, it emerges that bedforms are generally found on the gentle side of the scour, while the steep face is characterized by a more regular morphology (a selection of representative scour profiles is reported in Figure 5).

As shown in Figure 5, there is a clear relationship between the presence of bedforms and the scour slope (computed based on a 25-m running window along the transect). The along-scour slope reaches the maximum

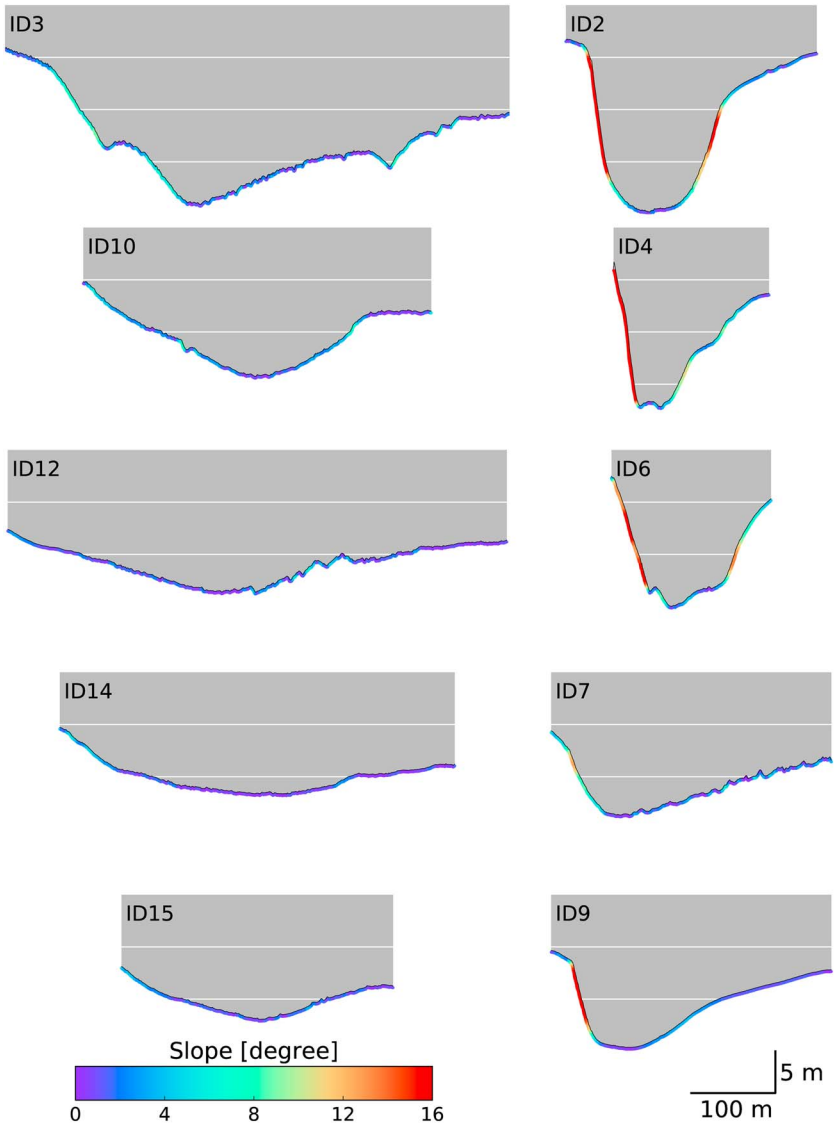

Figure 5. Cross sections at a number of confluence scours with the color of the bottom line indicating the bed slope. The white lines are spaced 5 m. All transects are oriented with the landward side on the left.

values of 35° at confluence scours ID2 and ID4. In general, there are no bedforms when the slopes bordering the scour hole have values larger than 8° – 10°.

Most of the scours in the Venice Lagoon have an asymmetric shape, with the steep face on the landward side (e.g., ID2, ID3, ID4, ID6, and ID7 in Figure 5). In some cases the confluence scour has a symmetric shape, with both sides characterized by a gentle slope (slope lower than 8° – 10°) and the presence of bedforms (e.g., ID10, ID12, ID14, and ID15 in Figure 5). This characteristic morphology is generated by the superposition of meander bend and confluence scour (ID10 and ID14) or adjacent confluence scours (ID12 and ID15).

3.3. Historical Bathymetries at Channel Confluences

For the analysis of the morphological evolution of confluence scours, we focused our investigation on two locations that are well described, in terms of bathymetric observations, by all available datasets. In the historical maps, the water depth measurements were concentrated in the main navigation channels and the inlets. We therefore selected the scour hole ID3, located at small distance from the Lido inlet (Figure 6), and the scour hole ID12 near the town (and inlet) of Chioggia (Figure 7).

The comparison of the different datasets allows us to follow the morphological evolution of the channel network over the past two centuries. While the shape of the channels joining confluence ID3 has not changed

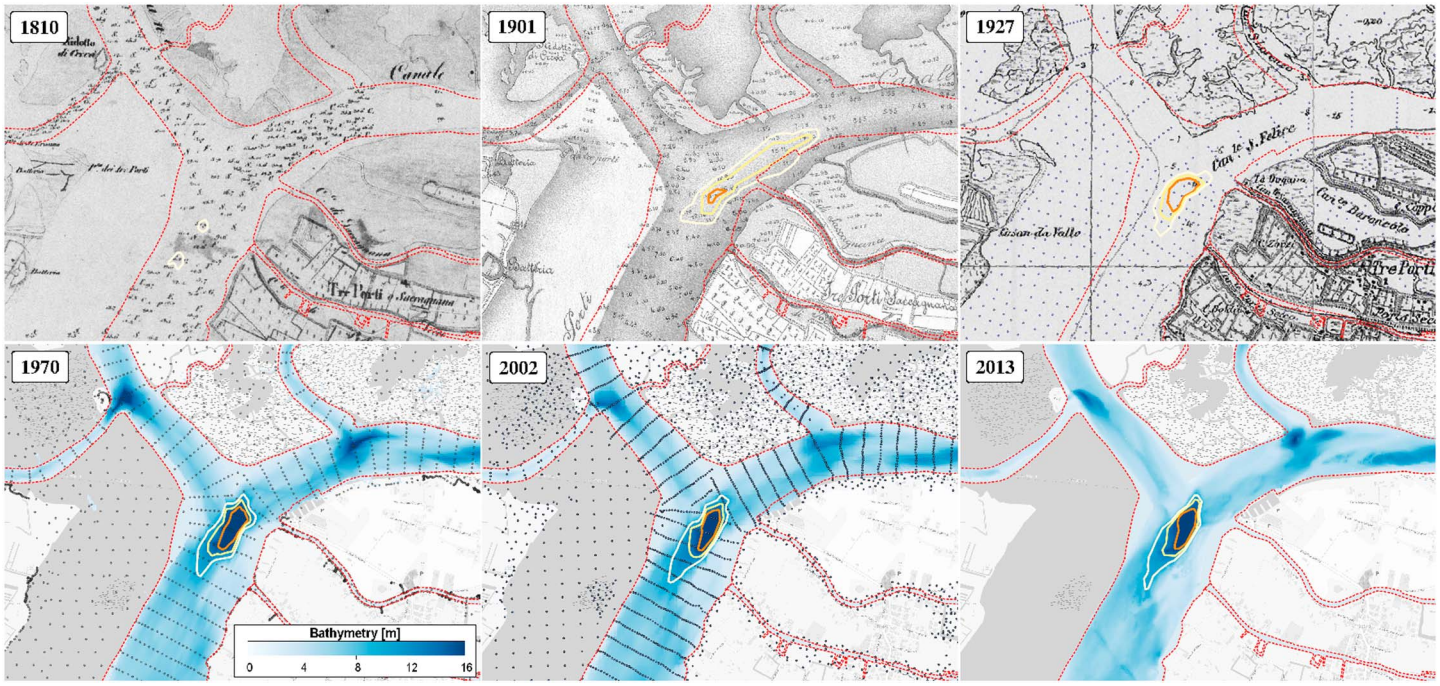

Figure 6. Confluence scour ID3 as represented by the available historical maps and bathymetric datasets. Depths reported in the 1810 map are in French feet (1 ft = 0.3248 m). Dots in maps 1927, 1970, and 2002 indicate the location of the available bathymetric stations. To outline the scour hole, the 10, 13, and 16-m isobaths are drawn with the yellow to orange contours, respectively. The red dashed lines indicate, as reference, the modern tidal channel boundaries. Background image from OpenStreetMap (http://www.openstreetmap.org).

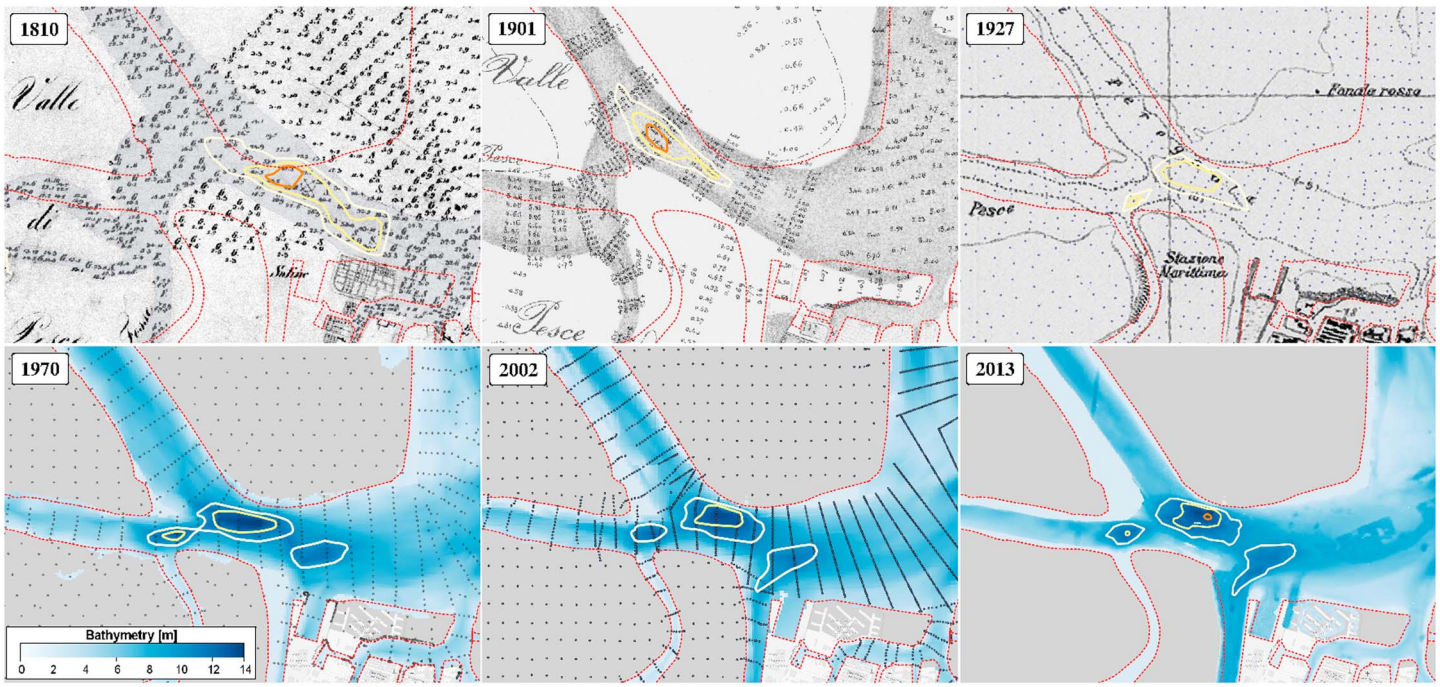

Figure 7. Same as Figure 6 for confluence scour ID12. To outline the scour hole, the 10-, 12-, and 14-m isobaths are drawn with the yellow to orange contours.

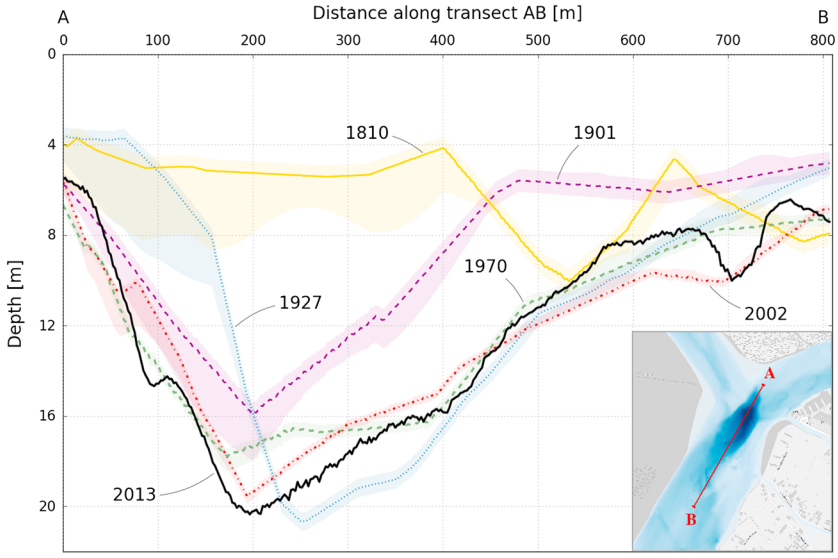

Figure 8. Comparison of depth profiles along the transect AB crossing scour hole ID3. Shadow represents the local uncertainty associated with the measurement technique and the interpolation process (see section 2.2).

significantly and remained confined by salt marshes (Figure 6), we cannot say the same for ID12. In the second case, the confluent unconfined channels migrated and changed form, a new channel was dredged along the western side of the city and the number of upstream tidal reaches changed over time (Figure 7). Figures 6 and 7 highlight the different number and position of the sparse bathymetric stations of the selected datasets. Generally, the observations were retrieved along cross-channel transects with an increasing number of measurements in the most recent surveys.

In order to analyze the major changes that occurred between 1810 and 2013, we extracted depth profiles along transects crossing the confluence scours ID3 (transect AB, Figure 8) and ID12 (transect CD, Figure 9), respectively. The local error has been computed as the sum of the errors associated with the measurement and the local deviation resulting from the interpolation procedure (shown by the shadowed envelope in Figures 8 and 9, with a 20-m centered moving average). The root-mean-square error along transect AB associated with the interpolation of the sparse observations was estimated as 2.2, 1.5, 1.8, 0.7, and 1.1 m for the 1810, 1901, 1927, 1970, and 2002 datasets, respectively. Along transect CD, the root-mean-square error was estimated

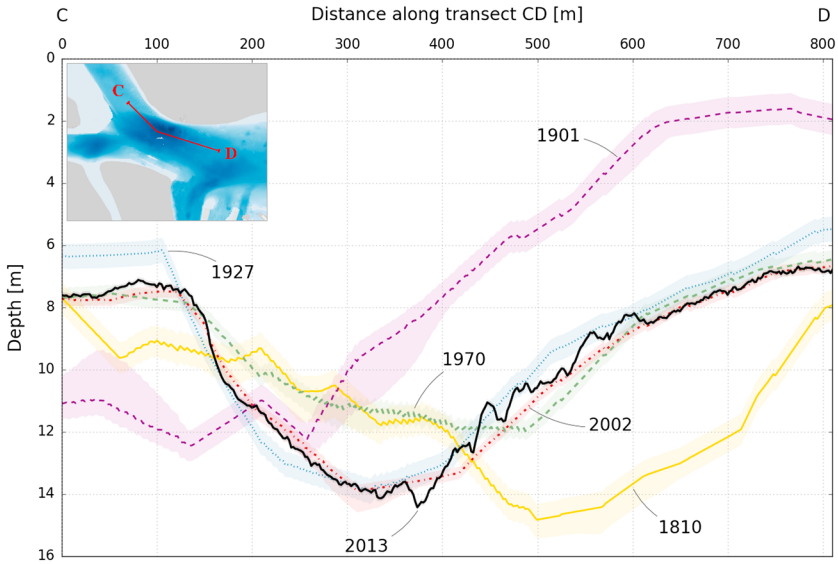

Figure 9. Same as Figure 8 but for transect CD crossing scour hole ID12.

as 0.6, 0.9, 0.3, 0.4, and 0.3 m for the same datasets. The errors associated with the interpolation of the sparse bathymetric points are higher than the ones (even exaggerated) of the vertical measuring technique.

At confluence ID3 the scour hole was not present in 1810. In 1901 it had an upstream elongated shape and a maximum depth exceeding 16 m (Figure 6). In the years to follow, the scour shrank and deepened, reaching a maximum depth of about 20 m in 1927. The subsequent bathymetric datasets reveal that the scour ID3 expanded downstream, with the maximum depth fluctuating between 18 and 20 m.

At confluence ID12, a scour could be identified in all datasets (Figures 7 and 9). Major changes occurred between 1810 and 1927, when the scour first migrated significantly landward (600 m from 1810 to 1901) and then back seaward (350 m from 1901 to 1927). From 1901 to 1927, a reduction of the angle of confluence between the tributary and main channel can be observed. Later, the scour depth and size remained almost stable. The migration of the tidal channels and the excavation of a new channel lead to the formation of a channel node with several reaches. As a consequence, a second (from 1927) and a third (from 1970) scour formed (see the 10-m isobath outlined by the light-yellow contour in Figure 7).

No substantial morphological alterations could be identified between 2002 and 2013 at the investigated channel confluences. Some bed modifications could be detected, especially at the confluence scour ID3 (Figures 6 and 8), but the low resolution of the 2002 dataset did not allow a more quantitative evaluation of the volumetric changes.

4. Discussion

4.1. Morphodynamics of Confluence Scours

According to several authors (Ashmore & Parker, 1983; Best, 1986, 1987, 1988; Best & Rhoads, 2008; Mosley, 1976; Sambrook Smith et al., 2005), the morphodynamics of river confluences is controlled by several factors: (i) the geometry of the confluence (i.e., the confluence angle), (ii) the bed height discordance between the main channel and the tributaries, (iii) the ratio of tributary and mainstream momentum flux, and (iv) any differences in density between the incoming flows. Here we discuss the possible impacts of these factors on the tidal channel junction morphology.

As shown in Figure 10, the scour holes in the tidal channels of the Venice Lagoon become generally deeper with increasing junction angle. However, the dataset exhibits a wide scatter, which can be attributed to other controlling factors, such as the number of tributaries, bed discordance and the characteristics of the incoming flow. A similar broad relationship between scour depth and junction angle was found for scours in the tidal creeks of coastal South Carolina (Kjerfve et al., 1979) and in rivers (Sambrook Smith et al., 2005). To enable a direct comparison with the fluvial environments, the river data retrieved from Figure 2 of Sambrook Smith et al. (2005) are plotted as blue triangles in Figure 10. Herein, to be consistent with the tidal channel morphology, we considered only field data of rivers with the upstream tributaries deeper than 1 m. The data comparison revealed that the values of the confluence angle and the relative scour depth for the scour holes of the Venice Lagoon channels are larger than those generally found in rivers (Ashmore & Parker, 1983; Best, 1986; Best & Rhoads, 2008; Sambrook Smith et al., 2005). Scours at tidal channel confluences have relative depths comparable to scours found at sharp bends in the Mahakam River in Indonesia (Vermeulen et al., 2014). Compared to the river data, the relation between confluence angle and relative scour depth is stronger in the presented data.

The three-dimensional flow structures at the channel confluence may be influenced by the depth difference between the two converging channels, with the development of helical cells and modification of the downstream mixing of the flow (Best & Roy, 1991; Ribeiro et al., 2012). It has been documented that, in river confluences with significant bed height discordance between the upstream channels, the tributary flow is generally confined to the upper part of the water column, whereas the main channel flow is deflected below it (Biron et al., 1996; De Serres et al., 1999; Ribeiro et al., 2012). Moreover, according to Sukhodolov et al. (2017), the flow within confluences with discordant beds and high-speed tributary flow can exhibit jet-like characteristics. Ten scour holes in the Venice Lagoon channels are found at the confluence of channels having a bed height discordance larger than 1 m. The maximum value of bed discordance is 6.1 m and is found in the deepest scour hole (ID1) located in the artificially dredged Malamocco-Marghera channel. In Venice Lagoon the relative scour depth is not correlated to the bed height discordance.

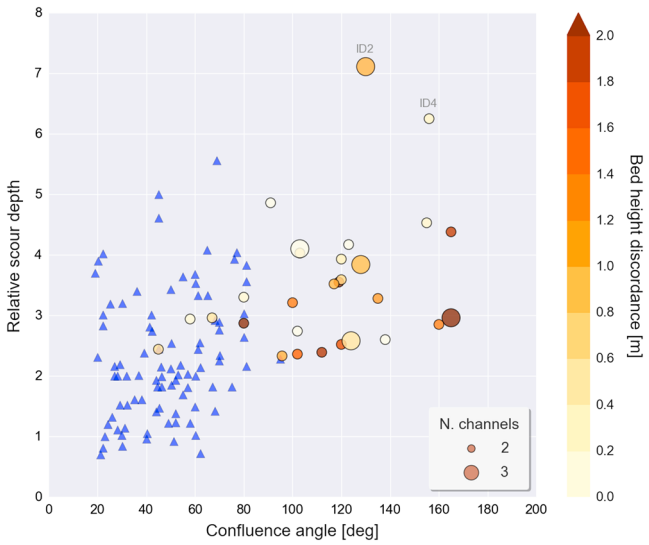

Figure 10. Relative scour depth (d_r) at the tidal channel junctions plotted against confluence angle in degrees. The size of the circles is proportional to the number of upstream channels, and the circle color represents the bed height discordance between the upstream channels. The blue triangles indicate river data from a range of studies, summarized by Sambrook Smith et al. (2005).

The water discharge of the streams joining a river confluence and their ratio have been identified as major factors controlling the flow structure and the morphology of confluence scours (Best, 1988; Best & Rhoads, 2008; Boyer et al., 2006; Constantinescu et al., 2014; De Serres et al., 1999; Mosley, 1982). In fluvial systems the channel morphodynamics can be modeled by considering only the characteristic discharge hypothesis (Paola et al., 1992). Similarly, in tidal channels, morphology and flow discharge are strongly correlated (O'Brien, 1969). The coupling between channel hydrodynamic and morphodynamic properties is usually empirically described by the tidal prism (P) and the channel cross-sectional area (A, computed with reference to the mean sea level) according to the geomorphic law:

$$A = xP^n \tag{2}$$

where the scaling coefficients x and n typically lie in the range $0.656–68{\cdot}10^{-4}$ and 0.74–1.0, respectively (Umgiesser et al., 2015). The tidal prism is defined as the volume of water that passes through the cross section in a half spring (i.e., maximum astronomical) tidal cycle. Even if originally the relationship was proposed for tidal inlets, its validity has been extended to the inner channels of Venice Lagoon (A. D'Alpaos et al., 2010; Umgiesser et al., 2015). To investigate the role of the channel discharge on scour morphology, we computed the tidal prism for all channels joining the confluences using the O'Brien (1969) relationship ($x = 0.656 \cdot 10^{-4}$ and $n = 1$) which, according to Umgiesser et al. (2015), best fits the channels of the Venice Lagoon. Figure 11 shows that the maximum scour depth is positively correlated to the tidal prism considered herein as the sum of the tidal prisms of the upstream reaches, with a coefficient of determination of 0.5. Therefore, as in rivers, generally the scour depth is related to the first-order scaling of channel geometry and discharge.

It should be noted that almost all scours having d_r higher than 4.0 are located in the northern lagoon at a remarkable distance from the Lido inlet (>10 km) along the channel system areas where most of the fresh water inputs of the Venice Lagoon are concentrated. The two scours with the highest relative depths, ID2 and ID4 with values of 7.1 and 6.2, respectively, receive waters directly from the Dese and Silone rivers. Figure 11 allows to discriminate two scours (ID2 and ID4) that can be considered as outliers with respect to general depth/tidal prism relationship. Therefore, these two scours could be dominated by local hydrodynamic processes, instead of being determined by the general scaling of the system.

According to Cheng and Valle-Levinson (2009) and Buschman et al. (2013), salinity differences, and therefore flow density gradients, play a role in controlling the scour hole dynamics. Cheng and Valle-Levinson (2009) found that during flood, when density decreases downflow, the maximum acceleration moves at the inland edge of the scour. In ebb phase instead, the density gradients tend to reduce velocities, particularly in the deepest part of the scour. Also Buschman et al. (2013) stressed the importance of the salinity vertical structure in flow definition, stating that the difference in the salinity of each channel provides modifications in the scour dynamics, affecting the sediment mobilization. At tidal junctions, salinity gradients can give rise to antiestuarine dynamics, creating vertical cells within the scour. Due to tidal straining (Simpson et al., 1990), vertical stratification in such systems is usually the strongest during ebb tide, when the flows of the upstream reaches converge to the confluence. Instead, strong mixing characterizes the flood phase, when the tidal flow coming from the inlet separates in the channel branches.

In tidally dominated systems, like the Venice Lagoon, the channel network departs from the inlets creating a dendritic or fractal structure (Hughes, 2012). The inlets govern the volume of water that enters and exits during each tidal cycle and that is fed into the lagoon through the channel network. Therefore, the tidal prism decreases going from the inlet to the inner lagoon (A. D'Alpaos et al., 2010). A general spatial trend was identified in the Venice Lagoon also for the depth of the scours, with the deepest holes generally found close to the inlets. Scours ID2 and ID4 are exceptions to this general rule. Their anomalous morphology can be explained, as discussed above, by the fact that hydrodynamics of these two confluences are probably influenced by flow density difference.

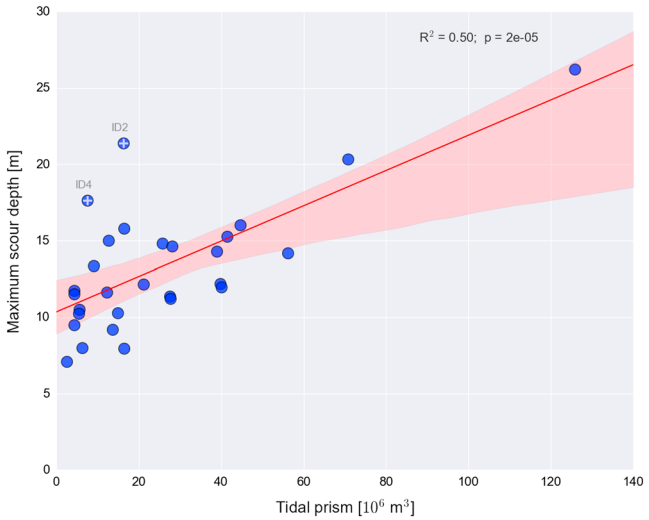

Figure 11. Maximum scour depth at the tidal channel junctions plotted against the total tidal prism of upstream channels. The regression line and the 95% confidence interval are plotted in red. Scours ID2 and ID4 are marked with white crosses.

The role of each factor on the morphodynamics of scours at tidal channel confluences was estimated by performing a multivariate correlation analysis between the scour depth values (both d_{max} and d_r) and the confluence angle, the bed height discordance between the upstream channels, the tidal prism and the ratio of tributary and mainstream discharge (i.e., tidal prism ratio). The analysis confirmed that the dominant influence on scour depth d_{max} is the tidal prism, explaining 43% of the variance, which goes up to 64% when ID2 and ID4 scours are excluded. Six percent of the variance in d_{max} is explained by the confluence angle. Among the considered factors, only the confluence angle and the discharge ratio play a significant role in controlling the d_r variability (13 and 11% of variance explained, respectively). Contrary to what is normally observed in rivers, we did not find an increase in the scour depth with increasing relative discharge of the tributary channel compared to the one of the mainstream (Best, 1988; Best & Rhoads, 2008; Boyer et al., 2006; Mosley, 1982).

Concluding, the major control of maximum scour depth seems to be the upstream tidal prism (i.e., the channel geometry, see equation (2) with only minor contributions from confluence geometry (confluence angle). However, it has to be noted that, generally, there is a high percentage (48% and 74% for d_{max} and d_r, respectively) of variance that is not correlated with any of the principal forcing. This is probably due to other factors, such as the flood/ebb alternation of the tidal flow, the local hydrodynamic processes at the confluence (influenced by density gradients between the channels), and the presence of the erosion-resistant clay layer, which, as found by Huismans et al. (2016) in the Rhine-Meuse Delta, could change the erodibility of the channel bed.

4.2. Bedforms and Sediment Dynamics at Channel Confluences

Unlike rivers, where the flow is unidirectional, in tidal channels erosion and deposition take place during the whole tidal cycle. As mentioned above, the high-resolution MBES bathymetry highlights the presence of small- and medium-scale bedforms on the gentle side of the scours. Conversely, bedforms are absent on the steep landward side of the scours. There gravity currents, vertical advection, and high macroscale turbulence induced by the diverging flow during flood tide (Cheng & Valle-Levinson, 2009; Kjerfve et al., 1979) may induce energetic flow entraining the sediment in suspension (Nittrouer et al., 2008), thus inhibiting the bedform formation.

According to Kjerfve et al. (1979) and Ginsberg and Perillo (1999), scours at tidal channel confluences are generally asymmetric, with ebb and flood currents dominating on the gentle (seaward) and steep (landward) slopes, respectively. Kjerfve et al. (1979) hypothesized that the formation of deep tidal scour holes is mainly due to hydraulic action primarily during the flood tide because of excessive macroscale turbulence, which is most intense at the steep side of the hole. Generally in the Venice Lagoon, the bedforms on the gentle seaward side are ebb oriented, indicating ebb dominance of the flow (Lefebvre et al., 2011). However, not all scours present bedforms on the gentle side (see, e.g., confluence scour ID9 in comparison to ID7). It is well known that the primary variables that affect bedform configuration and geometry in sandy tidal systems are the hydrodynamic forcing, flow depth, and sediment grain size (Ashley, 1990). However, in Venice Lagoon the bottom sediments are mainly composed of fine materials with the presence of sand only close to the inlets (Molinaroli et al., 2007). Therefore, seafloor features are expected to be influenced also by the sediment and biological cohesion (see review by Baas et al., 2016). Additionally, in the tidal channels of the Venice Lagoon a wide variety of benthic substrates was observed (such as bare muddy bottoms, patches of shell detritus, and sponges and macroalgal canopy on a bed of dead oysters), with altered seafloor roughness and sediment mobility (Montereale Gavazzi et al., 2016).

It is noteworthy that in symmetric scours, bedforms are ebb oriented on the seaward side and flood oriented on the landward side, indicating ebb and flood flow dominance on the seaward and landward side, respectively, thus confirming the finding of Kjerfve et al. (1979) and Ginsberg and Perillo (1999). Taking into account these findings and considering that the bathymetric data were acquired during all phases of the tidal cycle, we can affirm that bedform orientation does not change according to the instantaneous tidal currents, but reflects the dominant flow regime within the scour. This implies a limited mobility of bottom sediments.

Therefore, even if the tidal currents in the Venice Lagoon are ebb dominated (Ferrarin et al., 2015), the presence of flood-dominated bedforms indicates that the action of flood currents is relevant. The flood orientation of the bedforms on the landward side of the scour could be also due to vertical recirculation near the bed during ebb flow (MacVicar & Rennie, 2012).

A common bed feature at river confluences is the development of tributary mouth bars and downstream bars, corresponding to the accumulation of sediments at the mouth of one or both confluent channels, and to the convergence of sediment transport paths, respectively (Best, 1988; Best & Rhoads, 2008; Mosley, 1976). As in other tidal channel systems (Ginsberg & Perillo, 1999), these features were not found at channel confluences in the Venice Lagoon, probably due to the absence of sediment supply by the width-convergent channels. Indeed, the Venice Lagoon is a sediment-starved environment, since riverine sediment inputs into the lagoon have been drastically reduced (Sarretta et al., 2010; Zonta et al., 2005).

4.3. Long-Term Morphological Evolution of Confluence Scours

Considering the above findings, stating the role of the tidal currents in shaping the confluence scours, we discuss here the processes that induced the long-term morphological changes highlighted by comparing the historical bathymetric datasets. To this end, we have to consider that human interventions strongly altered the hydrodynamics in the tidal channel network (Carniello et al., 2009; L. D'Alpaos, 2010; L. D'Alpaos & Martini, 2005; Ferrarin et al., 2015; Tambroni & Seminara, 2006).

In 1810, no scour can be detected at confluence ID3, but two hollows were present south of the confluence. These erosive features can be interpreted as the troughs of a system of flood-oriented transverse dunes having a length of 325 m and a height of 5 m. The dune orientation indicates a flood-dominated system (Dronkers, 1986; Kwoll et al., 2014; Lefebvre et al., 2011), with a net sediment transport from the downstream channel toward the confluence. Probably, the net landward transport of sediments and the caranto layer, which in that area is located at depths between 10 and 14 m below sea level (Tosi et al., 2007a), prevented the formation of a scour hole at confluence ID3. On the other hand, the confluence scour ID12 (15-m deep in 1810) was probably always confined within the Holocene sediment package, without reaching the caranto, which has been estimated by Tosi et al. (2007b) to be between 16 and 18 m below sea level in this area.

It is reasonable to assume that major changes in the scour morphology between 1810 and 1901 can be related to the alteration of the Lido and Malamocco inlets. These modifications implied the unification of three ancient inlets with the construction of the jetties at Lido and the artificial stabilization of the Malamocco inlet with jetties (see Balletti, 2006, for a detailed reconstruction of the changes of the inlet morphology in the last two centuries). Consequently, the currents in the inlets and the adjacent channels became stronger, changed from flood dominated to ebb dominated, and the tidal discharge of the inlets increased considerably (L. D'Alpaos & Martini, 2005). This certainly had a strong impact on the morphology of confluence ID3, with the change of magnitude and direction of the net transport over a tidal cycle (Dronkers, 1986) and the downcutting below the overconsolidated clay layer caranto to about 16 m. A similar human-induced morphological evolution was found in the Rhine-Meuse Delta, where the alteration of the tidal regime, determined by the closure of the Haringvliet estuary with storm surge barriers in 1970, resulted in the incision of the clay layer and consequent development of scour holes (Hoitink et al., 2017; Huismans et al., 2016).

In 1901 the Lido and Malamocco inlets were already stabilized with jetties, while the Chioggia inlet was still unaltered. However, it must be stressed that in a multiple-inlet system, such as the Venice Lagoon, the flow in a given inlet may vary in response to the flow at all other inlets (Pacheco et al., 2010; Salles et al., 2005). The numerical analysis carried out by L. D'Alpaos and Martini (2005) on the 1811 and 1901 lagoon configurations, highlighted important changes in tidal current regime over the whole lagoon and in sea-lagoon exchanges at the three inlets. Indeed, the 1901 dataset indicates a significant deepening of most of the tidal channels also in the southern sector of the lagoon (L. D'Alpaos, 2010; Tambroni & Seminara, 2006). The migrations of confluence scour ID12 could therefore have been induced by the enhancement of the tidal flow regime determined by the artificial stabilization of the inlets with jetties. The mobility of the confluence is related to the active migration rates of the tidal channels, exceeding 10 m per century (Donnici et al., 2017). Similarly, the remarkable mobility of confluence scours induced by the modification of the flow regime is observed in many rivers (see review by Dixon et al., 2018), for example, in the Jamuna-Ganges junction (Bangladesh), where a 30-m-deep confluence scour migrated by 1.8 km during a monsoon flood period (Best & Ashworth, 1997).

For both investigated scours, we observed similar behavior: first, a decrease of the maximum scour depth of about 2.5 m between 1927 and 1970 (depositional phase) and then a subsequent deepening back to the 1927 level between 1970 and 2002 (erosional phase). In the last century, the Venice Lagoon underwent an extensive deepening as a consequence of sediment loss, with the strongest effects in the central basin (Sarretta et al., 2010). Our findings suggest that the fine sediments eroded in the tidal flats and salt marshes, first accumulated in the tidal channels and subsequently were transported out into the open sea. Such morphological processes could be accentuated by the excavation of the Malamocco-Marghera navigation channel in 1966–1969, which produced a permanent intensification of the tidal currents and alteration of the exchanges between the lagoon and the sea (Ferrarin et al., 2013) and exposed the channel margins and surrounding mudflats to the erosive action of ship wakes (Rapaglia et al., 2015; Zaggia et al., 2017).

From 2003 to 2012, the three inlets of the Venice Lagoon were subjected to further modifications for the construction of the system of mobile barriers (MoSE, from the Italian acronym for Experimental Electromechanical Module) for the defense of Venice and lagoon islands from floods caused by exceptional tides and storm surges. The reconfiguration of the inlets affected the tidal propagation in the lagoon (Ferrarin et al., 2015) and in the exchange between the lagoon and the sea (Ghezzo et al., 2010; Ferrarin et al., 2013). The comparison of bathymetries presented here indicates that these interventions did not produce significant changes in the geomorphology of the investigated scours.

The investigation of the historical datasets revealed the century-scale morphological dynamics of scours at tidal channel confluences. The studied erosive features develop within the Holocene deposits, cutting through the earlier low-stage deposits only in some cases. Their formation is expected to be related to the action of local (autocyclic) processes, such as tidal currents and associated turbulent structures. Similar to the scours found in the tidal creeks of coastal South Carolina (Kjerfve et al., 1979), it is thus unlikely that the holes are exhumed relict features. As in rivers, these erosive features likely leave unconformities in the sedimentary sequences (Best & Ashworth, 1997), having implications for the interpretation of scour surfaces in the stratigraphic record and reconstructions of past environmental changes (Dixon et al., 2018). However, the analysis presented herein shows that the potential areal extent of tidal channel confluence scour erosional surfaces is much lower (few hundreds of meters) than what is observed in large braided rivers (several kilometers, Dixon et al., 2018, and references therein). It is therefore improbable that these features can be mistaken with signatures driven by larger-scale allocyclic processes, such as sea-level changes. Further research is needed to determine the relative importance and the type of sedimentary geochemical and physical processes driving the scour morphodynamics, considering also that allocyclic forcing commonly induces changes in autocyclic processes (Cecil, 2003; Karamitopoulos et al., 2014).

5. Summary and Conclusions

Although there exists a large body of literature on confluence scours in rivers, the present research provides for the first time a comprehensive analysis of the morphological characteristics of scour holes at tidal channel junctions. This study is based on the analysis of high-resolution bathymetric data acquired in 2013 in the tidal channels of the Venice Lagoon with a multibeam echosounder system. The MBES acoustic mapping provided a detailed view of the three-dimensional properties of confluence scours. These observations reveal a wide variety of confluence planform geometries in terms of confluence angle and the number and shape of the channels joining the confluence. Similar to those found in rivers and other tidal systems, the shape of the scour holes at tidal channel confluences in the Venice Lagoon is generally asymmetric, with the steep face of the hole on the upstream edges of the junction zone where the contributing channels combine.

Generally, the tidal prism of the upstream channels is the major factor influencing the maximum scour depth. However, the presence of bed height discordance between the upstream channels, flood/ebb alternation of the tidal flow, and probably flow density difference leads to a large scatter in the morphological properties of the confluence scours identified in the Venice Lagoon channel network. The morphology of the confluence scour and its evolution are also affected by the presence of a subsurface bedrock (caranto) underlying the Holocene lagoonal deposits. The analysis of the seafloor roughness confirmed previous findings stating that in tidal channels both ebb and flood flows combine in shaping the confluence morphology, with ebb and flood currents dominating on the gentle and steep slopes, respectively.

These findings about geomorphology of scour holes will serve as a basis for future investigations of the complex hydrodynamic processes at tidal channel confluence. Following the methodologies applied in rivers

(Constantinescu et al., 2014; Li & Zheng, 2016; Sukhodolov et al., 2017; Vermeulen et al., 2015), the relative contribution of the different factors in controlling flow dynamics at channel confluences will be next evaluated using experimental data on currents and numerical models.

The analysis of historical datasets revealed that in the last two centuries the geomorphology of two investigated confluence scours changed significantly. The stabilization of the inlets with jetties and the excavation of new channels altered the general circulation in the lagoon and the dynamic morphological equilibrium of the tidal channels with evident impacts also on the confluence scour morphology. This analysis demonstrated that the tidal regime is the main driver of confluence scour formation and mobility. It will be crucial to repeat the high-resolution multibeam survey to track future changes in the geomorphology of scour holes and bedforms at tidal channel confluences.

The results of this study demonstrate that high-resolution mapping is of fundamental importance to improve our understanding of tidal channel morphodynamics. The recent technological development of bathymetric instruments allows the accurate exploration of the seafloor (Hughes Clarke, 2018), even in shallow water coastal systems (Madricardo & Rizzetto, 2018), which are among the areas most impacted by sea level rise and the direct effects of anthropic pressure. The present findings will thus be of general interest and demonstrate that integration of high-resolution seafloor mapping and morphological analysis, as proposed herein, can be adopted to investigate fluvial and tidal systems worldwide.

Acknowledgments
This research was funded by the Flagship Project RITMARE—The Italian Research for the Sea—coordinated by the Italian National Research Council and funded by the Italian Ministry of Education, University and Research within the National Research Program 2011–2013. The 2013 MBES bathymetric dataset is available at the Integrated Earth Data Applications (IEDA) repository (http://get.iedadata.org/doi/323605). The digital version of the historical maps and datasets are available at the Archive of Adriatic Studies (ASA, http://www.archiviostudiadriatici.it), the open access repository of books, papers, documents, and scientific collections (historical and modern) of the Institute of Marine Sciences (CNR-ISMAR) of Venice.

References

Ashley, G. M. (1990). Classification of large-scale subaqueous bedforms; A new look at an old problem. *International Journal of Sediment Research*, *60*(1), 160–172. https://doi.org/10.2110/jsr.60.160

Ashmore, P., & Parker, G. (1983). Confluence scour in coarse braided streams. *Water Resources Research*, *19*(2), 392–402. https://doi.org/10.1029/WR019i002p00392

Baas, J. H., Best, J. L., & Peakall, J. (2016). Predicting bedforms and primary current stratification in cohesive mixtures of mud and sand. *Journal of the Geological Society*, *173*(1), 12–45. https://doi.org/10.1144/jgs2015-024

Balletti, C. (2006). Digital elaborations for cartographic reconstruction: The territorial transformations of Venice harbours in historical maps. *e-Perimetron*, *1*(4), 274–286.

Balletti, C., Ceregato, A., Gottardi, C., Rizzi, F., & Vianello, A. (2016). 3D digitization and web publishing of an ISMAR cartographic heritage: Historical maps of Venice Lagoon. *e-Perimetron*, *11*(2), 47–56.

Best, J. L. (1986). The morphology of river channel confluences. *Progress in Physical Geography*, *10*(2), 157–174. https://doi.org/10.1177/030913338601000201

Best, J. L. (1987). Flow dynamics at river channel confluences: Implications for sediment transport and bed morphology. In F. G. Etheridge, R. M. Flores, & M. D. Harve (Eds.), *Recent developments in fluvial sedimentology, Special Publication* (pp. 27–35). Tulsa, OK: Society of Economic Paleontologists and Mineralogists.

Best, J. L. (1988). Sediment transport and bed morphology at river channel confluences. *Sedimentology*, *35*(3), 481–498. https://doi.org/10.1111/j.1365-3091.1988.tb00999.x

Best, J. L., & Ashworth, P. J. (1997). Scour in large braided rivers and the recognition of sequence stratigraphic boundaries. *Nature*, *287*, 275–277. https://doi.org/10.1038/387275a0

Best, J. L., & Rhoads, B. L. (2008). Sediment transport, bed morphology and the sedimentology of river channel confluences. In S. P. Rice, A. G. Roy, & B. L. Rhoads (Eds.), *River confluences, tributaries and the fluvial network* (pp. 45–72). Chichester, UK: John Wiley & Sons, Ltd. https://doi.org/10.1002/9780470760383ch4

Best, J. L., & Roy, A. G. (1991). Mixing-layer distortion at the confluence of channels of different depth. *Nature*, *350*, 411–413. https://doi.org/10.1038/350411a0

Biron, P., Roy, A. G., & Best, J. L. (1996). Turbulent flow structure at concordant and discordant open-channel confluences. *Experiments in Fluids*, *21*(6), 437–446. https://doi.org/10.1007/BF00189046

Biron, P., Roy, A. G., Best, J. L., & Boyer, C. J. (1993). Bed morphology and sedimentology at the confluence of unequal depth channels. *Geomorphology*, *8*(2), 115–129. https://doi.org/10.1016/0169-555X(93) 90032-W

Boyer, C., Roy, A. G., & Best, J. L. (2006). Dynamics of a river channel confluence with discordant beds: Flow turbulence, bed load sediment transport, and bed morphology. *Journal of Geophysical Research*, *111*, F04007. https://doi.org/10.1029/2005JF000458

Buschman, F. A., van der Vegt, M., Hoitink, A. J. F., & Hoekstra, P. (2013). Water and suspended sediment division at a stratified tidal junction. *Journal of Geophysical Research: Oceans*, *118*, 1459–1472. https://doi.org/10.1002/jgrc.20124

CARIS HIPS and SIPS (2013). User Guide v8.1.

Carniello, L., Defina, A., & D'Alpaos, L. (2009). Morphological evolution of the Venice lagoon: Evidence from the past and trend for the future. *Journal of Geophysical Research*, *114*, F04002. https://doi.org/10.1029/2008JF001157

Cecil, C. B. (2003). The concept of autocyclic and allocyclic controls on sedimentation and stratigraphy, emphasizing the climatic variable. In C. B. Cecil & N. T. Edgar (Eds.), *Climate controls on stratigraphy* (pp. 13–20). Tulsa, OK: SEPM (Society for Sedimentary Geology).

Cheng, P., & Valle-Levinson, A. (2009). Spatial variations of flow structure over estuarine hollows. *Continental Shelf Research*, *29*(7), 927–937. https://doi.org/10.1016/j.csr.2009.01.011

Constantinescu, G. S., Miyawaki, S., Rhoads, B. L., & Sukhodolov, A. N. (2014). Numerical evaluation of the effects of planform geometry and inflow conditions on flow, turbulence structure, and bed shear velocity at a stream confluence with a concordant bed. *Journal of Geophysical Research: Earth Surface*, *119*, 2079–2097. https://doi.org/10.1002/2014JF003244

D'Alpaos, L. (2010). L'evoluzione morfologica della Laguna di Venezia attraverso la lettura di alcune mappe storiche e delle sue carte idrografiche, Comune di Venezia, Istituzione Centro Previsioni e Segnalazioni Maree. in Italian.

D'Alpaos, A., Lanzoni, S., Marani, M., Fagherazzi, S., & Rinaldo, A. (2005). Tidal network ontogeny: Channel initiation and early development. *Journal of Geophysical Research*, *110*, F02001. https://doi.org/10.1029/2004JF000182

D'Alpaos, A., Lanzoni, S., Marani, M., & Rinaldo, A. (2010). On the tidal prism-channel area relations. *Journal of Geophysical Research*, *115*, F01003. https://doi.org/10.1029/2008JF001243

D'Alpaos, L., & Martini, P. (2005). The influence of the inlet configuration on sediment loss in the Venice Lagoon. In C. A. Fletcher & T. Spencer (Eds.), *Flooding and environmental challenges for Venice and its Lagoon: State of knowledge* (pp. 419–430). Cambridge, UK: Cambridge University Press.

De Marchi, L. (1913). Teoria degli scandagli d'alto mare (in Italian). *Memorie del R. Comitato Talassografico Italiano*, *31*, 1–41.

De Serres, B., Roy, A. G., Biron, P. M., & Best, J. L. (1999). Three-dimensional structure of flow at a confluence of river channels with discordant beds. *Geomorphology*, *26*(4), 313–335. https://doi.org/10.1016/S0169-555X(98)00064-6

Dixon, S. J., Sambrook Smith, G. H., Best, J. L., Nicholas, A. P., Bull, J. M., Vardy, M. E., et al. (2018). The planform mobility of river channel confluences: Insights from analysis of remotely sensed imagery, *176*, 1–18. https://doi.org/10.1016/j.earscirev.2017.09.009

Donnici, S., Madricardo, F., & Serandrei-Barbero, R. (2017). Sedimentation rate and lateral migration of tidal channels in the Lagoon of Venice (Northern Italy). *Estuarine, Coastal and Shelf Science*, *198*, 354–366. https://doi.org/10.1016/j.ecss.2017.02.016

Donnici, S., Serandrei-Barbero, R., Bini, C., Bonardi, M., & Lezziero, A. (2011). The caranto paleosol and its role in the early urbanization of Venice. *Geoarchaeology*, *26*(4), 514–543. https://doi.org/10.1002/gea.20361

Dronkers, J. (1986). Tidal asymmetry and estuarine morphology. *Journal of Sea Research*, *20*, 117–131. https://doi.org/10.1016/0077-7579(86)90036-0

Fagherazzi, S., Bortoluzzi, A., Dietrich, W. E., Adami, A., Lanzoni, S., Marani, M., & Rinaldo, A. (1999). Tidal networks: 1. Automatic network extraction and preliminary scaling features from digital terrain maps. *Water Resources Research*, *35*(12), 3891–3904. https://doi.org/10.1029/1999WR900236

Fagherazzi, S., Gabet, E. J., & Furbish, D. J. (2004). The effect of bidirectional flow on tidal channel planforms. *Earth Surface Processes and Landforms*, *29*(3), 295–309. https://doi.org/10.1002/esp.1016

Ferrarin, C., Cucco, A., Umgiesser, G., Bellafiore, D., & Amos, C. L. (2010). Modelling fluxes of water and sediment between the Venice Lagoon and the sea. *Continental Shelf Research*, *30*(8), 904–914. https://doi.org/10.1016/j.csr.2009.08.014

Ferrarin, C., Ghezzo, M., Umgiesser, G., Tagliapietra, D., Camatti, E., Zaggia, L., & Sarretta, A. (2013). Assessing hydrological effects of human interventions on coastal systems: Numerical applications to the Venice Lagoon. *Hydrology and Earth System Sciences*, *17*(5), 1733–1748. https://doi.org/10.5194/hess-17-1733-2013

Ferrarin, C., Tomasin, A., Bajo, M., Petrizzo, A., & Umgiesser, G. (2015). Tidal changes in a heavily modified coastal wetland. *Continental Shelf Research*, *101*, 22–33. https://doi.org/10.1016/j.csr.2015.04.002

Fraccascia, S., Winter, C., Ernstsen, V., & Hebbeln, D. (2016). Residual currents and bedform migration in a natural tidal inlet (Knudedyb, Danish Wadden Sea). *Geomorphology*, *271*, 74–83. https://doi.org/10.1016/j.geomorph. 2016.07.017

Ghezzo, M., Guerzoni, S., Cucco, A., & Umgiesser, G. (2010). Changes in Venice Lagoon dynamics due to construction of mobile barriers. *Coastal Engineering*, *57*(7), 694–708. https://doi.org/10.1016/j.coastaleng.2010.02.009

Ginsberg, S. S., Aliotta, S., & Lizasoain, G. O. (2009). Morphodynamics and seismostratigraphy of a deep hole at tidal channel confluence. *Geomorphology*, *104*(3-4), 253–261. https://doi.org/10.1016/j.geomorph.2008.09.002

Ginsberg, S. S., & Perillo, G. M. (1999). Deep-scour holes at tidal channel junctions, Bahia Blanca Estuary, Argentina. *Marine Geology*, *160*(1–2), 171–182. https://doi.org/10.1016/S0025-3227(99)00019-5

Hoitink, A. J. F., Wang, Z. B., Vermeulen, B., Huismans, Y., & Kästner, K. (2017). Tidal controls on river delta morphology. *Nature Geoscience*, *10*, 637–645. https://doi.org/10.1038/ngeo3000

Hooke, R. L., Martìn-Duque, J. F., & Pedraza, J. (2012). Land transformation by humans: A review. *GSA Today*, *22*(12), 4–10. https://doi.org/10.1130/GSAT151A.1

Hughes, Z. J. (2012). Tidal channels on tidal flats and marshes. In R. A. Davis Jr & R. W. Dalrymple (Eds.), *Principles of tidal sedimentology* (pp. 269–300). Dordrecht, The Netherlands: Springer. https://doi.org/10.1007/978-94-007-0123-6_11

Hughes Clarke, J. E. (2018). Multibeam Echosounders. In A. Micallef, S. Krastel, & A. Savini (Eds.), *Submarine geomorphology* (pp. 25–41). Cham, Switzerland: Springer International Publishing. https://doi.org/10.1007/978-3-319-57852-1_3

Huismans, Y., van Velzen, G., O'Mahoney, T., Hoffmans, G., & Wiersma, A. (2016). Scour hole development in river beds with mixed sand-clay-peat stratigraphy. In J. Harris, R. Whitehouse, & S. Moxon (Eds.), *Scour and erosion* (pp. 801–808). London, UK: CRC Press.

Karamitopoulos, P., Weltje, G. J., & Dalman, R. A. F. (2014). Allogenic controls on autogenic variability in fluvio-deltaic systems: Inferences from analysis of synthetic stratigraphy. *Basin Research*, *26*(6), 767–779. https://doi.org/10.1111/bre.12065

Keller, E. A. (1978). Pools, riffles, and channelization. *Environmental Geology*, *2*(2), 119–127. https://doi.org/10.1007/BF03804742

Kjerfve, B., Shao, C.-C., & Stapor, F. W. (1979). Formation of deep scour holes at the junction of tidal creeks: An hypothesis. *Marine Geology*, *33*(1), M9–M14. https://doi.org/10.1016/0025-3227(79)90126-9

Kwoll, E., Becker, M., & Winter, C. (2014). With or against the tide: The influence of bed form asymmetry on the formation of macroturbulence and suspended sediment patterns. *Water Resources Research*, *50*, 7800–7815. https://doi.org/10.1002/2013WR014292

Lefebvre, A., Ernstsen, V. B., & Winter, C. (2011). Influence of compound bedforms on hydraulic roughness in a tidal environment. *Ocean Dynamics*, *61*(12), 2201–2210. https://doi.org/10.1007/s10236-011-0476-6

Li, C., & Zheng, Q. (2016). Breakdown of hydrostatic assumption in tidal channel with scour holes. *Frontiers in Marine Science*, *3*, 199. https://doi.org/10.3389/fmars.2016.00199

MacVicar, B. J., & Rennie, C. D. (2012). Flow and turbulence redistribution in a straight artificial pool. *Water Resources Research*, *48*, W02503. https://doi.org/10.1029/2010WR009374

Madricardo, F., & Donnici, S. (2014). Mapping past and recent landscape modifications in the Lagoon of Venice through geophysical surveys and historical maps. *Anthropocene*, *6*, 86–96. https://doi.org/10.1016/j.ancene.2014.11.001

Madricardo, F., Foglini, F., Kruss, A., Ferrarin, C., Pizzeghello, N. M., Murri, C., et al. (2017). High-resolution multibeam and hydrodynamic datasets of tidal channels and inlets of the Lagoon of Venice. *Scientific Data*, *4*, 170121. https://doi.org/10.1038/sdata.2017.121

Madricardo, F., & Rizzetto, F. (2018). Shallow coastal landforms. In A. Micallef, S. Krastel, & A. Savini (Eds.), *Submarine geomorphology* (pp. 161–183). Cham, Switzerland: Springer International Publishing. https://doi.org/10.1007/978-3-319-57852-1_10

Madricardo, F., Tgowski, J., & Donnici, S. (2012). Automated detection of sedimentary features using wavelet analysis and neural networks on single beam echosounder data: A case study from the Venice Lagoon, Italy. *Continental Shelf Research*, *43*, 43–54. https://doi.org/10.1016/j.csr.2012.04.018

Magrini, G. (1933a). Atlante Primo.: Carta topografica idrografica militare della laguna di Venezia rilevata dal capitano Augusto Denaix negli anni 1809-10-11. In G. Magrini (Ed.), *La Laguna di Venezia*. Venezia, Italia: Magistrato delle Acque, Ufficio del Genio Civile di Venezia, Carlo Ferrari. in Italian.

Magrini, G. (1933b). *Atlante Terzo.: Riproduzione della Carta topografica - idrografica militare della laguna di Venezia e del litorale compreso tra l'Adige e il Sile eseguita per ordine del Ministero dei Lavori Pubblici dall'Ufficio del Genio Civile di Venezia negli anni 1897 e 1901*. in Italian.

Maselli, V., & Trincardi, F. (2013). Man made deltas. *Science Reports*, *3*, 1926. https://doi.org/10.1038/srep01926
Molinaroli, E., Guerzoni, S., Sarretta, A., Cucco, A., & Umgiesser, G. (2007). Links between hydrology and sedimentology in the Lagoon of Venice, Italy. *Journal of Marine Systems*, *68*(3-4), 303–317. https://doi.org/10.1016/j.jmarsys.2006.12.003
Montereale Gavazzi, G., Madricardo, F., Janowski, L., Kruss, A., Blondel, P., Sigovini, M., & Foglini, F. (2016). Evaluation of seabed mapping methods for fine-scale classification of extremely shallow benthic habitats—Application to the Venice Lagoon, Italy. *Estuarine, Coastal and Shelf Science*, *170*, 45–60. https://doi.org/10.1016/j.ecss.2015.12.014
Mosley, M. P. (1976). An experimental study of channel confluences. *The Journal of Geology*, *84*, 535–562.
Mosley, M. P. (1982). Scour depths in branch channel confluences, Ohau River, Otago, New Zealand. *Transactions of the Institution of Professional Engineers New Zealand: Civil Engineering Section*, *9*, 17–24.
Nittrouer, J. A., Allison, M. A., & Campanella, R. (2008). Bedform transport rates for the lowermost Mississippi River. *Journal of Geophysical Research*, *113*, F03004. https://doi.org/10.1029/2007JF000795
O'Brien, M. P. (1969). Equilibrium flow areas of inlets in sandy coasts. *Journal of the Waterways, Harbors, and Coastal Engineering Division American Society of Civil Engineers*, *95*, 43–52.
Pacheco, A., Ferreira, O., Williams, J. J., Garel, E., Vila-Concejo, A., & Dias, J. A. (2010). Hydrodynamics and equilibrium of a multiple-inlet system. *Marine Geology*, *274*(1), 32–42. https://doi.org/10.1016/j.margeo.2010.03.003
Paola, C., Heller, P. L., & Angevine, C. L. (1992). The large-scale dynamics of grain-size variation in alluvial basins, 1: Theory. *Basin Research*, *4*(2), 73–90. https://doi.org/10.1111/j.1365-2117.1992.tb00145.x
Pérez-Ruzafa, A., Marcos, C., & Pérez-Ruzafa, I. (2011). Mediterranean coastal lagoons in an ecosystem and aquatic resources management context. *Physics and Chemistry of the Earth*, *36*(5–6), 160–166. https://doi.org/10.1016/j.pce.2010.04.013
Perillo, G. M. E., Wolanski, E., Cahoon, D. R., & Brinson, M. M. (2009). *Coastal wetlands: An integrated ecosystem approach*. Amsterdam, The Netherlands: Elsevier.
Pierini, J. O., Perillo, G. M. E., Carbone, M. E., & Marini, F. M. (2005). Residual flow structure at a scour-hole in Bahia Blanca Estuary, Argentina. *Journal of Coastal Research*, *21*(4), 784–796. https://doi.org/10.2112/010-NIS.1
Rapaglia, J., Zaggia, L., Parnell, K., Lorenzetti, G., & Vafeidis, A. T. (2015). Ship-wake induced sediment remobilization: Effects and proposed management strategies for the Venice Lagoon. *Ocean and Coastal Management*, *110*, 1–11. https://doi.org/10.1016/j.ocecoaman.2015.03.002
Rhoads, B. L., Lewis, Q. W., & Andresen, W. (2016). Historical changes in channel network extent and channel planform in an intensively managed landscape: Natural versus human-induced effects. *Geomorphology*, *252*, 17–31. https://doi.org/10.1016/j.geomorph.2015.04.021
Ribeiro, L., Blanckaert, M. K., Roy, A. G., & Schleiss, A. J. (2012). Flow and sediment dynamics in channel confluences. *Journal of Geophysical Research*, *117*, F01035. https://doi.org/10.1029/2011JF002171
Rice, S. P., Roy, A. G., & Rhoads, B. L. (2008). *River confluences, tributaries and the fluvial network*. Chichester, UK: John Wiley. https://doi.org/10.1002/9780470760383
Riley, J. D., & Rhoads, B. L. (2012). Flow structure and channel morphology at a natural confluent meander bend. *Geomorphology*, *163–164*, 84–98. https://doi.org/10.1016/j.geomorph.2011.06.011
Riley, J. D., Rhoads, B. L., Parsons, D. R., & Johnson, K. K. (2015). Influence of junction angle on three-dimensional flow structure and bed morphology at confluent meander bends during different hydrological conditions. *Earth Surface Processes and Landforms*, *40*(2), 252–271. https://doi.org/10.1002/esp.3624
Rizzetto, R., Tosi, L., Brancolini, G., Baradello, L., & Tang, C. (2009). Ancient geomorphological features in shallows of the Venice Lagoon (Italy). *Journal of Coastal Research*, *SI56*, 752–756.
Roberts, M. V. T. (2004). Flow dynamics at open channel confluent-meander bends (Master's thesis), University of Leed, Leeds, U. K.
Salas-Monreal, D., & Valle-Levinson, A. (2009). Continuously stratified flow dynamics over a hollow. *Journal of Geophysical Research*, *114*, C03021. https://doi.org/10.1029/2007JC004648
Salles, P., Voulgaris, G., & Aubrey, D. G. (2005). Contribution of nonlinear mechanisms in the persistence of multiple tidal inlet systems. *Estuarine, Coastal and Shelf Science*, *65*(3), 475–491. https://doi.org/10.1016/j.ecss.2005.06.018
Sambrook Smith, G. H., Ashworth, P. J., Best, J. L., Woodward, J., & Simpson, C. J. (2005). The morphology and facies of sandy braided rivers: Some considerations of scale invariance. In M. Blum, S. Marriott, & S. Leclair (Eds.), *Fluvial Sedimentology VII* (pp. 145–158). Oxford, UK: Blackwell Publishing Ltd. https://doi.org/10.1002/9781444. pages={304350}ch9
Sarretta, A., Molinaroli, E., Guerzoni, S., Fontolan, G., & Pillon, S. (2010). Sediment budget in the Lagoon of Venice. *Continental Shelf Research*, *30*(8), 934–949. https://doi.org/10.1016/j.csr.2009.07.002
Simpson, J. H., Brown, J., Matthews, J., & Allen, G. (1990). Tidal straining, density currents, and stirring in the control of estuarine stratification. *Estuaries*, *13*(2), 125–132. https://doi.org/10.2307/1351581
Storms, J. E., Weltje, G. J., Terra, G. J., Cattaneo, A., & Trincardi, F. (2008). Coastal dynamics under conditions of rapid sea-level rise: Late Pleistocene to Early Holocene evolution of barrier-lagoon systems on the northern Adriatic shelf (Italy). *Quaternary Science Reviews*, *27*(11–12), 1107–1123. https://doi.org/10.1016/j.quascirev.2008.02.009
Sukhodolov, A. N., Krick, J., Sukhodolova, T. A., Cheng, Z., Rhoads, B. L., & Constantinescu, G. S. (2017). Turbulent flow structure at a discordant river confluence: Asymmetric jet dynamics with implications for channel morphology. *Journal of Geophysical Research: Earth Surface*, *122*, 1278–1293. https://doi.org/10.1002/2016JF004126
Syvitski, J. P. M., Kettner, A. L., Overeem, I., Hutton, E. W. H., Hannon, M. T., Brakenridge, R., et al. (2009). Sinking deltas due to human activities. *Nature Geoscience*, *2*, 681–686. https://doi.org/10.1038/ngeo629
Tambroni, N., & Seminara, G. (2006). Are inlets responsible for the morphological degradation of Venice Lagoon? *Journal of Geophysical Research*, *111*, F03013. https://doi.org/10.1029/2005JF000334
Tosi, L., Rizzetto, F., Bonardi, M., Donnici, S., Serandrei-Barbero, R., & Toffoletto, R. (2007a). Note illustrative della Carta Geologica d'Italia alla scala 1:50.000, foglio 128 Venezia, SystemCart APAT, Dipartimento Difesa del Suolo, Servizio Geologico d'Italia. (pp. 1–164). in Italian.
Tosi, L., Rizzetto, F., Bonardi, M., Donnici, S., Serandrei-Barbero, R., & Toffoletto, R. (2007b). Note illustrative della Carta Geologica d'Italia alla scala 1:50.000, foglio 148-149 Chioggia-Malamocco, SystemCart APAT, Dipartimento Difesa del Suolo, Servizio Geologico d'Italia. 1–164, in Italian.
Umgiesser, G., Helsby, R., Amos, C. L., & Ferrarin, C. (2015). Tidal prism variation in Venice Lagoon and inlet response over the last 70 years. In G. Umgiesser, R. Helsby, C. L. Amos, & C. Ferrarin (Eds.), *Sediment fluxes in coastal areas, coastal research library* Vol. 10, pp. 151–165). Netherlands: Springer. https://doi.org/10.1007/978-94-017-9260-8_7
Umgiesser, G., Melaku Canu, D., Cucco, A., & Solidoro, C. (2004). A finite element model for the Venice Lagoon. Development, set up, calibration and validation. *Journal of Marine Systems*, *51*, 123–145. https://doi.org/10.1016/j.jmarsys.2004.05.009
Van Rijn, L. C. (1998). *Principles of coastal morphology*. Amsterdam, The Netherlands: Aqua Publications.

Vermeulen, B., Hoitink, A. J. F., Berkum, S. W., & Hidayat, H. (2014). Sharp bends associated with deep scours in a tropical river: The river Mahakam (East Kalimantan, Indonesia). *Journal of Geophysical Research: Earth Surface*, *119*, 1441–1454. https://doi.org/10.1002/2013JF002923

Vermeulen, B., Hoitink, A. J. F., & Labeur, R. J. (2015). Flow structure caused by a local cross-sectional area increase and curvature in a sharp river bend. *Journal of Geophysical Research: Earth Surface*, *120*, 1771–1783. https://doi.org/10.1002/2014JF003334

Wolanski, E., & Elliott, M. (2015). *Estuarine ecohydrology. An introduction*. Amsterdam, The Netherlands: Elsevier.

Wright, D. J., Pendleton, M., Boulware, J., Walbridge, S., Gerlt, B., Eslinger, D., et al. (2012). ArcGIS Benthic Terrain Modeler (BTM), v. 3.0 (Technical Report). Boston, MA: Environmental Systems Research Institute, NOAA Coastal Services Center, Massachusetts Office of Coastal Zone Management.

Zaggia, L., Lorenzetti, G., Manfé, G., Scarpa, G. M., Molinaroli, E., Parnell, K. E., et al. (2017). Fast shoreline erosion induced by ship wakes in a coastal lagoon: Field evidence and remote sensing analysis. *PLOS ONE*, *12*(10), 1–23. https://doi.org/10.1371/journal.pone.0187210

Zecchin, M., Baradello, L., Brancolini, G., Donda, F., Rizzetto, F., & Tosi, L. (2008). Sequence stratigraphy based on high-resolution seismic profiles in the late Pleistocene and Holocene deposits of the Venice area. *Marine Geology*, *253*(3), 185–198. https://doi.org/10.1016/j.margeo.2008.05.010

Zille, G. G. (1955). I rilievi geodetici, topografici ed idrografici della Laguna dalla fine del Secolo XVIII ai giorni nostri. In R. Cessi, G. Bunelli, U. D'Ancona, L. Vollo, & G. G. Zille (Eds.), *La Laguna di Venezia* (Vol. 1, pp. 35–87). Venezia, Italia: CIESM, Carlo Ferrari. in Italian.

Zonta, R., Collavini, F., Zaggia, L., & Zuliani, A. (2005). The effect of floods on the transport of suspended sediments and contaminants: A case study from the estuary of the Dese River (Venice Lagoon, Italy). *Environment International*, *31*, 948–958.